SAMTEC TR 78-101

A PRELIMINARY STUDY OF

SAMTEC POSTFLIGHT REFRACTION CORRECTION

Federal Electric Corporation
Vandenberg AFB, Calif. 93437

31 JUL 78

UMLIMITED DISTRIBUTION

Prepared for

SPACE AND MISSILE TEST CENTER
Vandenberg AFB, Calif. 93437

This final report was submitted by Federal Electric Corporation, Vandenberg AFB, CA 93437 under Contract F04703-77-C-0111 with the Space and Missile Test Center, Vandenberg AFB, CA 93437. Operations Research Analyst, Mr R. Lane, XRQA, was the Division Project Engineer-in-Charge.

This report has been reviewed by the Information Office (OI) and is releasable to the National Technical Information Service (NTIS). At NTIS, it will be available to the general public, including foreign nations.

This technical report has been reviewed and is approved for publication.

Richard Lane

RICHARD LANE GS-14
Project Engineer

EUGENE E. CLARY GS-15
Chief, Requirements & Evaluation Division

FOR THE COMMANDER

Robert E. Foster

ROBERT E. FOSTER, Colonel, USAF
Director of Plans, Programs & Resources

SECURITY CLASSIFICATION OF THIS PAGE (When Data Entered)

REPORT DOCUMENTATION PAGE	READ INSTRUCTIONS BEFORE COMPLETING FORM
1. REPORT NUMBER: SAMTEC TR-78-101	2. GOVT ACCESSION NO. / 3. RECIPIENT'S CATALOG NUMBER
4. TITLE (and Subtitle): A Preliminary Study of SAMTEC Postflight Refraction Correction	5. TYPE OF REPORT & PERIOD COVERED: Final rept 1 may [redacted]-31 Jul 78
	6. PERFORMING ORG. REPORT NUMBER: PA 100-77-55A
7. AUTHOR(s): R. Y. Han	8. CONTRACT OR GRANT NUMBER(s): Space and Missile Test Cntr Contract F04703-77-C-0111
9. PERFORMING ORGANIZATION NAME AND ADDRESS: Federal Electric Corporation, PO Box 1886, Vandenberg Air Force Base, CA 93437	10. PROGRAM ELEMENT, PROJECT, TASK AREA & WORK UNIT NUMBERS: 78032F
11. CONTROLLING OFFICE NAME AND ADDRESS: Space and Missile Test Center (AFSC), Code XRQ, Vandenberg Air Force Base, CA 93437	12. REPORT DATE: 31 Jul 78 / 13. NUMBER OF PAGES: 101
14. MONITORING AGENCY NAME & ADDRESS (if different from Controlling Office): N/A	15. SECURITY CLASS. (of this report): UNCLASSIFIED / 15a. DECLASSIFICATION/DOWNGRADING SCHEDULE

16. DISTRIBUTION STATEMENT (of this Report)

UNLIMITED DISTRIBUTION (14) PA 100-77-55A

17. DISTRIBUTION STATEMENT (of the abstract entered in Block 20, if different from Report)

UNLIMITED DISTRIBUTION

18. SUPPLEMENTARY NOTES

19. KEY WORDS (Continue on reverse side if necessary and identify by block number)

Refraction
Radar

20. ABSTRACT (Continue on reverse side if necessary and identify by block number)

Refraction correction is one of the important steps in metric data processing. The purpose of this refraction study is to investigate the current postflight refraction correction technique which is applied to SAMTEC radar data obtained from missile and aircraft tracking. This study serves as a preliminary step for future development to establish the minimum acceptable operational criteria on refraction corrections to meet range user's data accuracy requirements. In this task the following were investigated: the differences between refraction

DD FORM 1 JAN 73 1473 EDITION OF 1 NOV 65 IS OBSOLETE

SECURITY CLASSIFICATION OF THIS PAGE (When Data Entered)

corrections based on the rawinsonde profile and several model profiles, the errors in refraction corrections based on rawinsonde-measured profiles and the minimum height required for rawinsonde measurements.

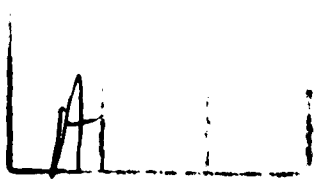

TABLE OF CONTENTS

		Page
	LIST OF FIGURES	*iii*
	LIST OF TABLES	*v*
1.0	INTRODUCTION	1
2.0	PROCEDURE FOR GENERATING REFRACTION CORRECTIONS	3
	2.1 Collection of Rawinsonde Data	3
	2.2 Generation of Refractivity Profile	6
	2.3 Calculations of Refraction Corrections	10
3.0	DIFFERENCES BETWEEN REFRACTION CORRECTIONS BASED ON RAWINSONDE PROFILE AND SELECTED MODEL PROFILES	12
	3.1 Comparison of the Refractivity Profiles	12
	3.2 Comparison of the Refraction Corrections	18
	3.3 Summary	24
4.0	ERRORS IN REFRACTION CORRECTIONS BASED ON MEASURED RAWINSONDE DATA	25
	4.1 Errors in the Collected Rawinsonde Data	27
	4.2 Errors in the Refractivity Profiles	27
	4.2.1 Errors Propagated from Rawinsonde Data	27
	4.2.2 Errors Introduced in Processing	32
	4.2.3 Refractivity Profiles with Errors	34
	4.3 Errors in the Refraction Corrections	34
	4.3.1 Errors Propagated from the Measured Profile	34
	4.3.2 Errors Introduced in Computation	42
	4.4 Errors Due to Space Variation	42
	4.5 Permissible Refraction Correction Errors for SAMTEC Radars	44
	4.6 Summary	44

TABLE OF CONTENTS (Continued)

		Page
5.0	MINIMUM HEIGHT REQUIRED FOR RAWINSONDE MEASUREMENTS	50
	5.1 Errors Due to Incomplete Rawinsonde Measurements	50
	5.2 Temporal Variations of Refractivity Profiles	54
	5.3 Summary	59
6.0	CONCLUSIONS AND SUGGESTIONS	60
	6.1 Conclusions	60
	6.2 Suggestions For Future Study	61
	REFERENCES	62
	APPENDICES	
	A: TABULATED REFRACTION CORRECTIONS BASED ON RAWINSONDE PROFILES AND SELECTED REFRACTIVITY MODELS	63
	B: TABULATED METEOROLOGICAL PARAMETERS AND REFRACTIVITY ERRORS	68
	C: TABULATED ERRORS IN REFRACTION CORRECTIONS	75
	D: PERMISSIBLE REFRACTION CORRECTION ERRORS FOR SAMTEC RADARS	81
	E: TABULATED REFRACTION CORRECTIONS BASED ON THE PROFILES WITH DIFFERENT CUTOFF HEIGHTS	87

FIGURES

Figure		Page
2.1	Generation of Refractivity Profile	8
3.1	The Refractivity Profile Obtained from Rawinsonde Measurements and Selected Model Profiles (Vandenberg, Op 6290, July 15, 1976)	14
3.2	The Refractivity Profile Obtained from Rawinsonde Measurements and Selected Model Profiles (Pillar Point, Op 6290, July 15, 1976)	16
3.3	The Refractivity Profile Obtained from Rawinsonde Measurements and Selected Model Profiles (Vandenberg, Op. 3445, January 21, 1977)	19
3.4	The Refractivity Profile Obtained from Rawinsonde Measurements and Selected Model Profiles (Pillar Point, Op. 3445, January 21, 1977)	21
4.1	The Relationship Among Various Error Sources	26
4.2	Errors in Refractivity Profile Obtained from Rawinsonde Measurements (Vandenberg, Op. 6290, July 15, 1976)	35
4.3	Errors in Refractivity Profile Obtained from Rawinsonde Measurements (Pillar Point, Op. 6290, July 15, 1976)	37
4.4	The Errors of Refraction Correction for Range (Op. 6290, Radar 213002)	40
4.5	The Errors of Refraction Correction for Elevation Angle (Op. 6290, Radar 213002)	41
4.6	Total Refraction Correction Errors (Op. 6290, Radar 213002)	49
5.1	Comparison of Total Refraction Correction Errors Derived from Complete and Incomplete Rawinsonde Profiles (Op. 6290, Radar 213002)	53

FIGURES (Continued)

Figure		Page
5.2	Refractivity Profiles Measured by Rawinsondes Launched at Vandenberg in Summer	55
5.3	Refractivity Profiles Measured by Rawinsondes Launched at Vandenberg in Winter	57

TABLES

Table		Page
2.1	Mandatory Pressure Levels for Synoptic Weather Analyses	4
2.2	Typical Rawinsonde Launch Schedule for Supporting Missile Launches and Synoptic Analyses	5
3.1	The Percentage Errors in the Total Corrections	23
3.2	Worst Case Refraction Correction Errors	23
4.1	Data Reliability of Meteorological Parameters	28
4.2	Results of the Comparisons made for Different Refraction Correction Programs	43
4.3	Differences in Refraction Corrections Versus Flight Time Rawinsonde Minus REFRACTOMETER for the Vandenberg Radar	45
4.4	Differences in Refraction Corrections Versus Flight Time Rawinsonde Minus REFRACTOMETER for the Pillar Point Radar	46
4.5	Estimated Percentages of Various Residual Refraction Correction Errors	47
A.1	The Differences Between the Refraction Corrections Based on Rawinsonde Profile and Model Profiles (Radar 023003, Vandenberg, Op 6290, July 15, 1976)	64
A.2	The Differences Between the Refraction Corrections Based on Rawinsonde Profile and Model Profiles (Radar 213002, Pillar Point, Op 6290, July 15, 1976)	65
A.3	The Differences Between the Refraction Corrections Based on Rawinsonde Profile and Model Profiles (Radar 023003, Vandenberg, Op 3445, January 21, 1977)	66
A.4	The Differences Between the Refraction Corrections Based on Rawinsonde Profile and Model Profiles (Radar 213002, Pillar Point, Op 3445, January 1977)	67

TABLES (Continued)

Table		Page
B.1	Meteorological Parameters, Refractivity, and the Errors at Significant Levels from Rawinsonde Measurements at Vandenberg for Op. 6290	69
B.2	Meteorological Parameters, Refractivity, and the Errors at Significant Levels from Rawinsonde Measurements at Point Pillar for Op. 6290	71
B.3	Refractivity Errors Caused by Uncertainties in Temperature, Water Vapor, and Pressure Measurements at Vandenberg for Op. 6290	73
B.4	Refractivity Errors Caused by Uncertainties in Temperature, Water Vapor, and Pressure Measurements at Point Pillar for Op. 6290	74
C.1	Errors in Refraction Corrections Based on Rawinsonde Measurements (Radar 213002, Pillar Point, Op. 6290, July 15, 1976)	76
C.2	Errors in Refraction Corrections Based on Rawinsonde Measurements (Radar 023003, Vandenberg, Op. 6290, July 15, 1976)	78
C.3	Errors in Refraction Corrections Based on Rawinsonde Measurements (Radar 213002, Pillar Point, Op. 3445, January 21, 1976)	79
C.4	Errors in Refraction Corrections Based on Rawinsonde Measurements (Radar 023003, Vandenberg, Op 3445, January 21, 1977)	80
D.1	The RMS and Averages of Residual Errors for SAMTEC Radars	83

TABLES (Continued)

Table		Page
E.1	The Differences Between Refraction Corrections Based on the Profiles with Different Cutoff Heights and the Original Profile (Radar 023003, Vandenberg, Op. 6290, July 15, 1976)	88
E.2	The Differences Between Refraction Corrections Based on the Profiles with Different Cutoff Heights and the Original Profile (Radar 213002, Pillar Point, Op. 6290, July 15, 1976)	92

1.0 INTRODUCTION

Refraction correction is one of the important steps in metric data processing. The purpose of refraction correction is to determine and correct for the errors introduced in radar tracking by propagation of electromagnetic waves through the atmosphere. There are two regions in this non-homogenous medium which can cause refraction to the electromagnetic waves propagating through it. They are the lower atmosphere and the ionosphere. The refractive medium of the lower atmosphere consists of the neutral molecules which can be polarized by the radiowave propagating through it. This region extends from ground to 120,000 ft which includes the troposphere and the stratosphere. The most important part for refraction is the troposphere. Therefore, the refraction caused by the region is often referred to as tropospheric refraction. The refractive medium of the ionosphere is composed of the ions and the free electrons. This refractive region extends from approximately 270,000 ft up to 3,000,000 ft. The major part of the region for refraction is near the peak of F_2 layer, which is between 900,000 and 1,500,000 ft.

The purpose of this refraction study is to investigate the current postflight refraction correction technique which is applied to SAMTEC radar data obtained from missile and aircraft tracking. This study will serve as a preliminary step for future development to establish the minimum acceptable operational criteria on refraction corrections to meet range users' data accuracy requirements. The current postflight data reduction procedure does not include the ionospheric refraction corrections. The current lower-atmosphere refraction corrections on range, elevation angle, and range rate are generated from the rawinsonde-measured atmospheric parameters —— pressure, temperature, and relative humidity. There is no refraction correction for azimuth angle in the current postflight data processing; meteorological measurements are insufficient to give any useable variation of refractivity versus azimuth.

The specific topics covered in this report are a result of the investigations of the following subjects:

(1) Differences between refraction corrections based on the rawinsonde profile and some model profiles.

(2) Errors in refraction corrections based on rawinsonde measurements.

(3) The minimum height required for rawinsonde measurements.

These three topics are to be discussed in terms of the sensor-centered coordinates (range and elevation angle) for individual radars. Because of the limited manhour level of effort applied to this task and the nature of the computer runs involved, there was no attempt to perform the multisensor BET calculations in the study to determine the sensitivity of the trajectory to the refraction corrections for various configurations of sensor tracking assignments. Based on the results obtained in this study, however, the effect of the refraction corrections on the multi-sensor BET solution can be investigated in a follow-on task.

Before looking into the specific topics, it is important to first understand the current preferred procedure for generating refraction corrections, which includes the following three steps:

(1) Collection of the raw data measured by rawinsonde,

(2) Generation of the refractivity profile from rawinsonde data, and

(3) Calculation of refraction corrections based on the refractivity profile generated from rawinsonde measurements.

2.0 PROCEDURE FOR GENERATING REFRACTION CORRECTIONS

2.1 Collection of Rawinsonde Data

The type of rawinsonde launched from Vandenberg AFB and Pillar Point AFS is AN/AMT-4. This type of rawinsonde has a balloonborne instrument package which contains a temperature sensor (thermistor), a relative humidity sensor (hygristor), and a pressure sensor (aneroid). The balloon also carries a L-band transmitter. As the balloon rises the aneroid pressure sensor expands and mechanically moves a contact arm across two interleaved sets of finger contacts alternately sensing the temperature and humidity measurements for transmission. The switching rate is indicative of the pressure change. In effect temperature and humidity measurements are multiplexed at a rate proportional to pressure change.

The ground system used for tracking and receiving signals is AN/GMD-1, which uses a parabolic autotracking antenna to measure the azimuth and elevation angles of the balloon. This system does not have the capability to make range measurements.

Three different sets of raw data tabulated from rawinsonde measurements are those of the one-minute levels, the mandatory levels, and the significant levels. The data set of one-minute levels is primarily needed for generating wind velocity and direction, while combined with the azimuth and elevation data which are recorded at one-minute intervals. The mandatory levels are the fixed pressure levels as specified in Table 2.1. The significant levels are the boundaries of strata having differing temperature lapse rates or vertical humidity gradients. The data of mandatory levels and significant levels are used for synoptic analyses at Department of Defense and civilian weather centers. The data of one-minute and the significant levels are used for range support. A typical schedule of rawinsonde launches at Vandenberg AFB and Pillar Point AFS is given in Table 2.2.

Table 2.1 Mandatory Pressure Levels for Synoptic Weather Analyses

Surface
1000 mb
850 mb
700 mb
500 mb
400 mb
300 mb
250 mb
200 mb
150 mb
100 mb
70 mb
50 mb
30 mb
20 mb
10 mb
7 mb
5 mb
3 mb
2 mb
1 mb

Table 2.2 Typical Rawinsonde Launch Schedule for Supporting Missile Launches and Synoptic Analyses

Time of launch (hours)	Place of launch*	Purpose of launch
T-20 to T-10	NV	For preflight weather information
T-8 to T-5	NV	For GO/NO GO decision
T-3	SV	Fast rising balloon for GO/NO GO decision, launched only when necessary
T-0	SV	For postflight
T-0	PP	refraction corrections
00 (- 1 hr. 45 min., + 1 hr.) (GMT)	NV	For synoptic
12 (- 1 hr. 45 min., + 1 hr.) (GMT)	NV	analyses

* NV = North Vandenberg
SV = South Vandenberg
PP = Pillar Point

The regular procedure to launch the rawinsonde and to collect data is as follows:

(1) The sensors are checked and calibrated by putting the whole instrument package into the Baseline Check Box, which is equipped with a psychrometer. The calibration scales for temperature and relative humidity measurements are set on the stripchart. A Baroswitch Pressure Calibration Chart supplied for each aneroid by the manufacturer is used for calibration of the pressure measurement.

(2) The battery used in the instrument package is charged.

(3) The balloon is filled with helium. The amount of the gas filled into the balloon will determine the maximum altitude which the balloon can reach. The lifting force of the balloon is checked against a fixed weight.

(4) The balloon is released and the dish antenna is operated to track the balloon.

(5) The significant levels are labeled on the stripchart by the operators. The speed of the stripchart is one inch per minute. The ordinate readings of temperature and relative humidity and the corresponding contact point numbers of pressure for the significant, one-minute, and mandatory levels are manually recorded on a Computer Data Worksheet.

(6) The elevation and azimuth angles of the balloon are automatically recorded once per minute for later processing to generate wind information.

(7) The data recorded on the Computer Data Worksheet is punched on paper tape and is either transmitted to ETR (Patrick AFB, Florida) or input to the local NOVA 1220 minicomputer for further processing. The data transmitted to ETR are composed of the one-minute levels and the significant levels. The data input to the local computer are from the sets of mandatory levels and significant levels.

2.2 Generation of Refractivity Profile

The data transmitted to ETR is processed by the Program RAWI on the CDC Cyber 74 computer. This program is written in FORTRAN IV language. It is a standard IRIG rawinsonde data reduction program [1]. This program accepts the data of the one-minute and significant levels and processes

the data to generate the height and the corresponding refractivity for each level. The interpolation from one-minute levels to the height levels with 1000 - foot interval is also handled by this program. Figure 2.1 is an illustration of the relations among various physical quantities involved in this processing. The mathematical steps are summarized as follows:

1. The temperature and relative humidity ordinate readings with the corresponding contact point numbers of each level are first converted into the temperature (°C), relative humidity (%), and pressure (mb) by using the calibration scales and chart.

2. The absolute vapor pressure (mb) is calculated from the relative humidity (%) by using the following empirical formula

$$E = RH \cdot 6.11 \cdot 10^{\left(\frac{7.5T}{237.3 + T}\right)} \tag{2.1}$$

where T = temperature (°C)
RH = relative humidity (%)
E = vapor pressure (mb)

3. The virtual temperature is calculated:

$$TV = \frac{TK}{1.0 - 0.379 \frac{E}{P}} \tag{2.2}$$

where TV = virtual temperatue at current level (°K)
TK = temperature (°K)
P = total pressure of the current level (mb)

and

$$TVB = \frac{TV + TVP}{2}$$

where TVB = mean virtual temperature (°K)
TVP = virtual temperature at previous level (°K)

4. The geopotential height of the data point is computed by assuming the hydrostatic equilibrium. The equation used for this computation is

$$HGT = HGTP + \left[\text{Log}_{10}\left(\frac{PP}{P}\right) \cdot HV \cdot TVB\right] \tag{2.3}$$

(A) COMPUTATION OF REFRACTIVITY

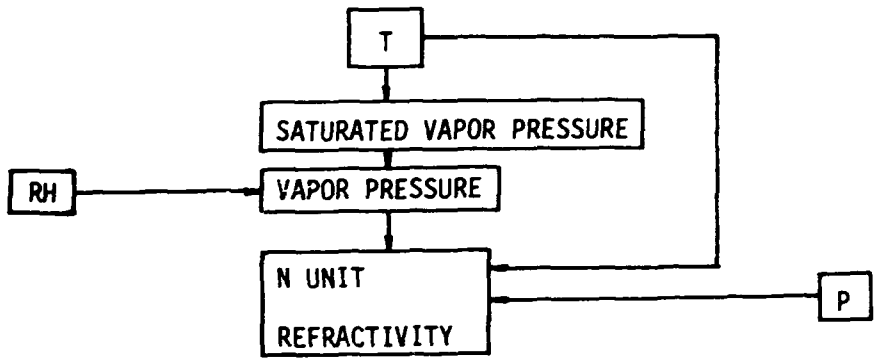

(B) COMPUTATION OF HEIGHT

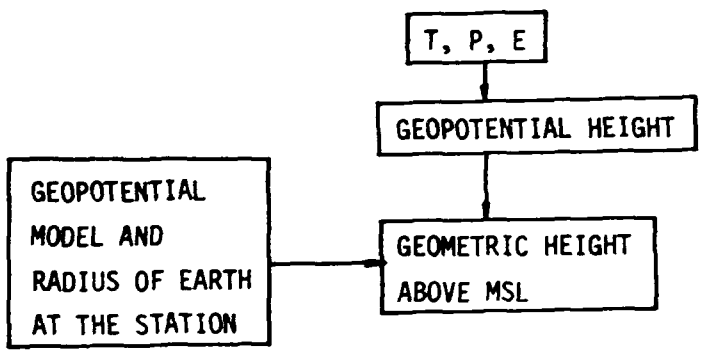

FIGURE 2.1 GENERATION OF REFRACTIVITY PROFILE

where PP = pressure of previous level (mb)

HV = 221.266 for computations in feet or 67.442 for computations in meters.

HGTP = geopotential height of previous level.

5. The geometric height is computed from the geopotential height,

$$Z = \frac{GARR \cdot HGT}{GRRA - HGT} \tag{2.4}$$

where GRRA = the combined gravitational and radius of the earth factor for station latitude.

GARR = the radius of the earth factor for station latitude.

6. The refractivity in N units is calculated by the following formula,

$$RI = [(77.6\ P) - (11.0\ E) + \frac{374808\ E}{TK}]\ (TINV) \tag{2.5}$$

where $TINV = \frac{1}{TK}$

RI = refractivity (N units)

7. The values of temperature, relative humidity, and refractivity at the height levels of 1000-foot interval can be linearly interpolated from the values of one-minute levels, respectively, by using the equation

$$X = X(2) - (\frac{Z(2) - HS}{Z(2) - Z(1)})\quad (X(2) - X(1)) \tag{2.6}$$

where Z(2) = the altitude of the upper data level,

Z(1) = the altitude of the lower data level,

HS = the altitude of interest

X(2) = the value of the parameter at Z(2)

X(1) = the value of the parameter at Z(1)

X = the interpolated value of the parameter at HS.

Meanwhile, the values of pressure can be logarithmically interpolated by the following equation,

$$X = 10^{[\text{Log } X(2) - \frac{Z(2) - HS}{Z(2) - Z(1)} (\text{Log } X(2) - \text{Log } X(1))]} \qquad (2.7)$$

The data processed locally at Vandenberg AFB is first handled by the National Weather Service Synoptic Program (NWSS Program). The input required by this program are the data of the mandatory and significant levels. The processed data output from this program are fed into another program for interpolation of data points at the height levels with 1000 - foot interval. The basic mathematical techniques used locally are the same as those used at ETR.

2.3 Calculations of Refraction Corrections

In the postflight data reduction process, the tropospheric refraction corrections for SAMTEC radar data are generated by using the PFDR Program module, called REFRC [2], on the Sigma 7 computer or by the Program NTABLE, on the IBM 7094 computer. This is a FORTRAN IV routine in double precision. Applying ray tracing technique to a given refractivity profile, this module can calculate the true range and elevation angle of a target from radar measurements. It may also compute the apparent range and elevation angle from true position parameters. The ray tracing technique in this module assumes a spherically stratified atmosphere with layers concentric with the earth center. The refractivity is assumed to vary linearly between the boundaries of a layer. The altitudes of the boundaries of each layer and the corresponding values of refractivity are input directly or provided by the Central Radio Propagation Laboratory (CRPL) exponential model profile [2, 13] contained in the program module.

The CRPL exponential model profile is extrapolated from a given surface refractivity value and will be explained in detail in Section 3.0. The input refractivity profile is primarily taken from the data set of significant levels. The refractivity data points of the 1000 - foot levels are only used to intervene with that part of the significant - level data above 15,000 ft when the change of refractivity between two consecutive significant levels is larger than 12 N units.

The mathematics used in this program module to generate the refraction corrections on range and elevation angle are described in detail in the documents [3, 11, 12]. The refraction correction for range rate is computed by another PFDR program module, called SMOOVA. In this module a second-degree polynomial is fitted by least-square method to a sliding span of 5.0 seconds (51 data points) of the range refraction correction. The first time derivative of the polynomial is taken as the refraction correction for range rate. The data rates for refraction corrections on range, elevation angle, and range rate are 10 pps. The corrections are applied to the data in the following way:

$$R_{corrected} = R_{observed} - DR$$

$$E_{corrected} = E_{observed} - DE$$

$$\dot{R}_{corrected} = \dot{R}_{observed} - \dot{DR}$$

where DR, DE, and $\dot{DR}$ are the refraction corrections on range, elevation angle, and range rate, respectively.

3.0 DIFFERENCES BETWEEN REFRACTION CORRECTIONS BASED ON RAWINSONDE PROFILE AND SELECTED MODEL PROFILES

In this section the refraction corrections derived from the rawinsonde profile and several model profiles are compared in an attempt to explore a better model which can be used if rawinsonde measurements are not available.

3.1 Comparison of the Refractivity Profiles

Two model refractivity profiles were compared with the profiles generated from rawinsonde measurements. The first one is the CRPL exponential model extrapolated from the surface refractivity value. The second one is an annual mean profile for the Vandenberg area.

The annual mean profile was derived from the combination of the long-term observations from Vandenberg AFB and the IRIG documented data for Point Arguello, California. This profile is available in the SAMTEC Default Meteorological File, which can be obtained from Metric Data Reduction Department of FEC.

The exponential model was developed by the Central Radio Propagation Laboratory [2, 13] and was implemented in the REFRC module of the postflight data reduction program. If the input of the refractivity data to the REFRC module is only a surface value, an exponential profile will be generated based on this input surface refractivity. This model has the following mathematical form,

$$N = N_s \, e^{-C_e(h - h_s)} \tag{3.1}$$

where h = altitude above mean sea level (km),

N = refractivity at altitude h,

h_s = surface elevation above mean sea level (km),

N_s = surface refractivity value at h_s,

C_e = a constant factor which determines the rate of decay of N with h. (km^{-1}).

The coefficient C_e should be determined by both the surface refractivity value and the refractivity value at 1 km above the surface, that is,

$$C_e = \ln \frac{N_S}{N \text{ (1 km above surface)}} \quad (km^{-1})$$

$$= \ln \frac{N_S}{N_S + \Delta N} \tag{3.2}$$

where $\Delta N = N \text{ (1 km)} - N_S$

According to some statistical analysis based on long-term observations, the value of ΔN can be best approximated by the following formula,

$$\Delta N = -7.32 \exp (0.005577\ N_S) \tag{3.3}$$

Therefore, once N_S is known, the profile can be obtained by using Equations (3.1), (3.2), and (3.3).

In order to compare the refraction corrections based on the model profiles with those computed with the measured profiles, two MM III operations were selected in this study. Op 6290 with a 33 degree reentry angle was conducted on July 15, 1976 whereas the missile of Op 3445 with a 22 degree reentry angle was launched on January 21, 1977. The rawinsonde profiles obtained for these two operations can be used to represent the two extreme seasonal weather conditions, the summer and the winter.

The rawinsonde refractivity profiles measured at Vandenberg and Pillar Point for Op 6290 are plotted together with the two model profiles in Figures 3.1 and 3.2. The comparison of these profiles can be best described in four regions. Below 2000 ft the exponential and the measured profiles are very close to each other. In the region between 2000 and 15,000 ft, there exists the most significant difference between the two kinds of profiles. In this region the rawinsonde profiles have abrupt decreases with the altitude due to the existence of temperature inversion layer. The exponential model cannot show the existence of any layer. The refractivities of the exponential profiles are larger than those of the rawinsonde in this region. The differences can be as large as 60 N units. The altitude of 15,000 ft is a crossing point, above which the refractivities of rawinsonde profiles

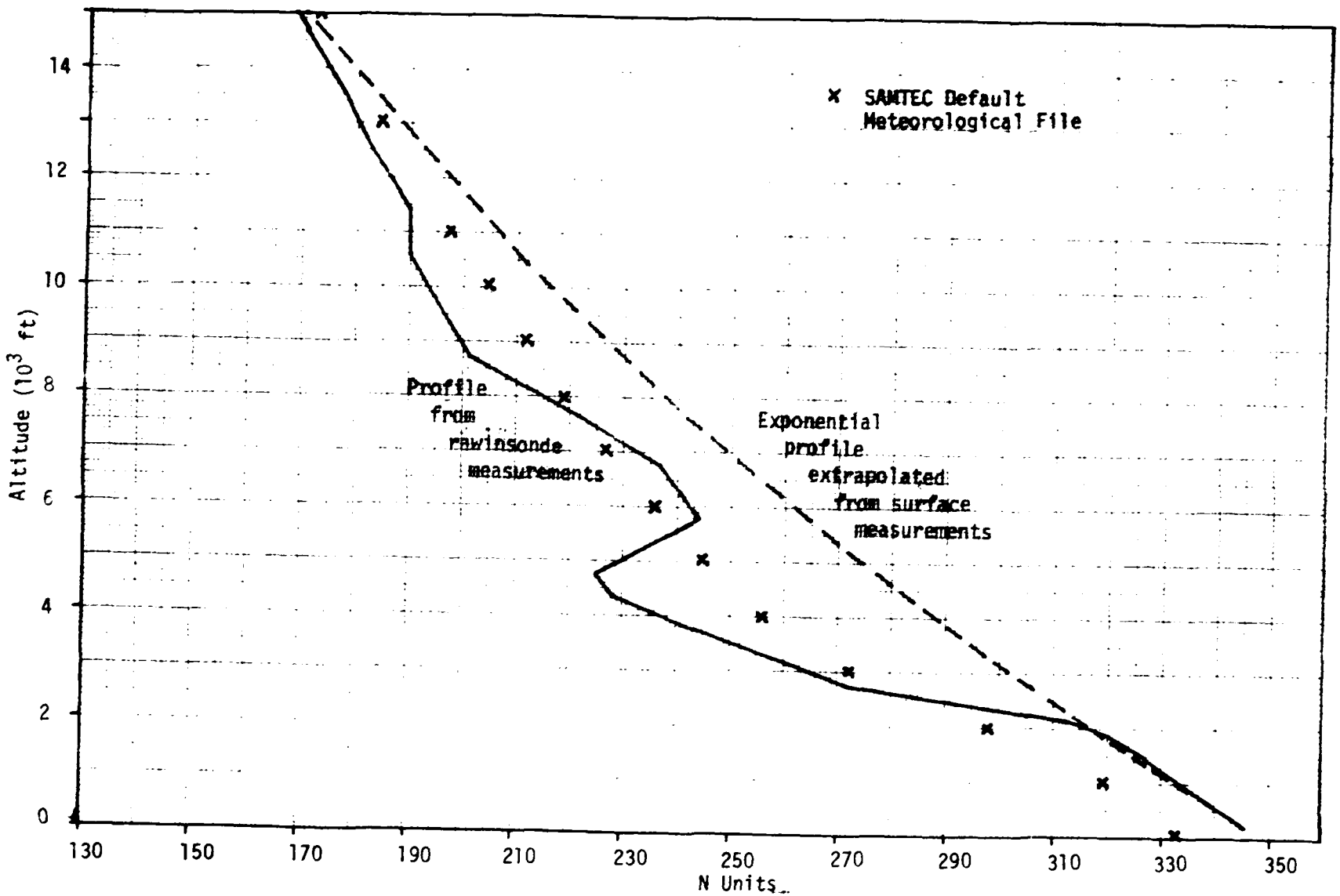

Figure 3.1 The refractivity profile obtained from rawinsonde measurements and selected model profiles (Vandenberg, Op. 6290, July 15, 1976)

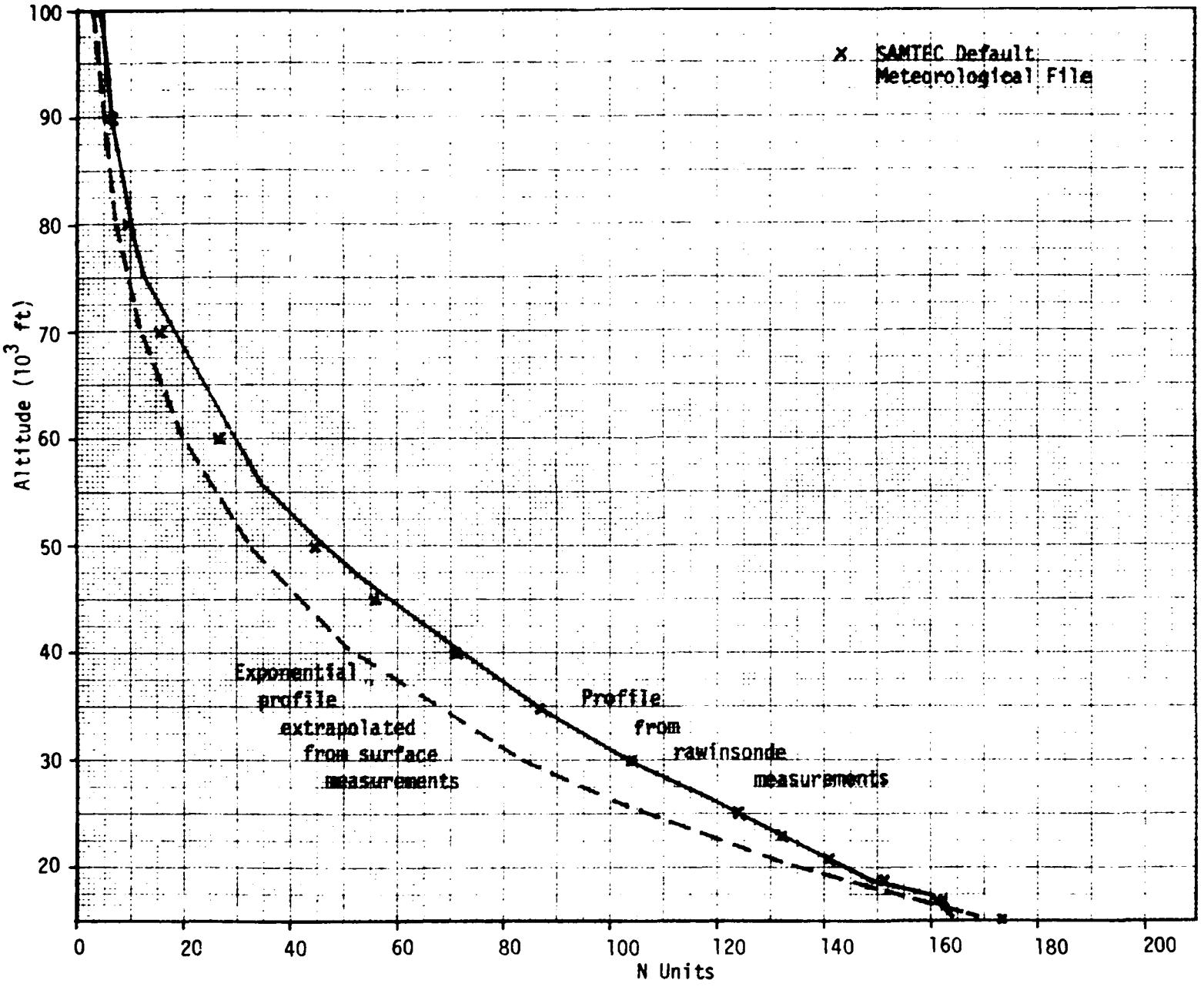

Figure 3.1 (Continued)

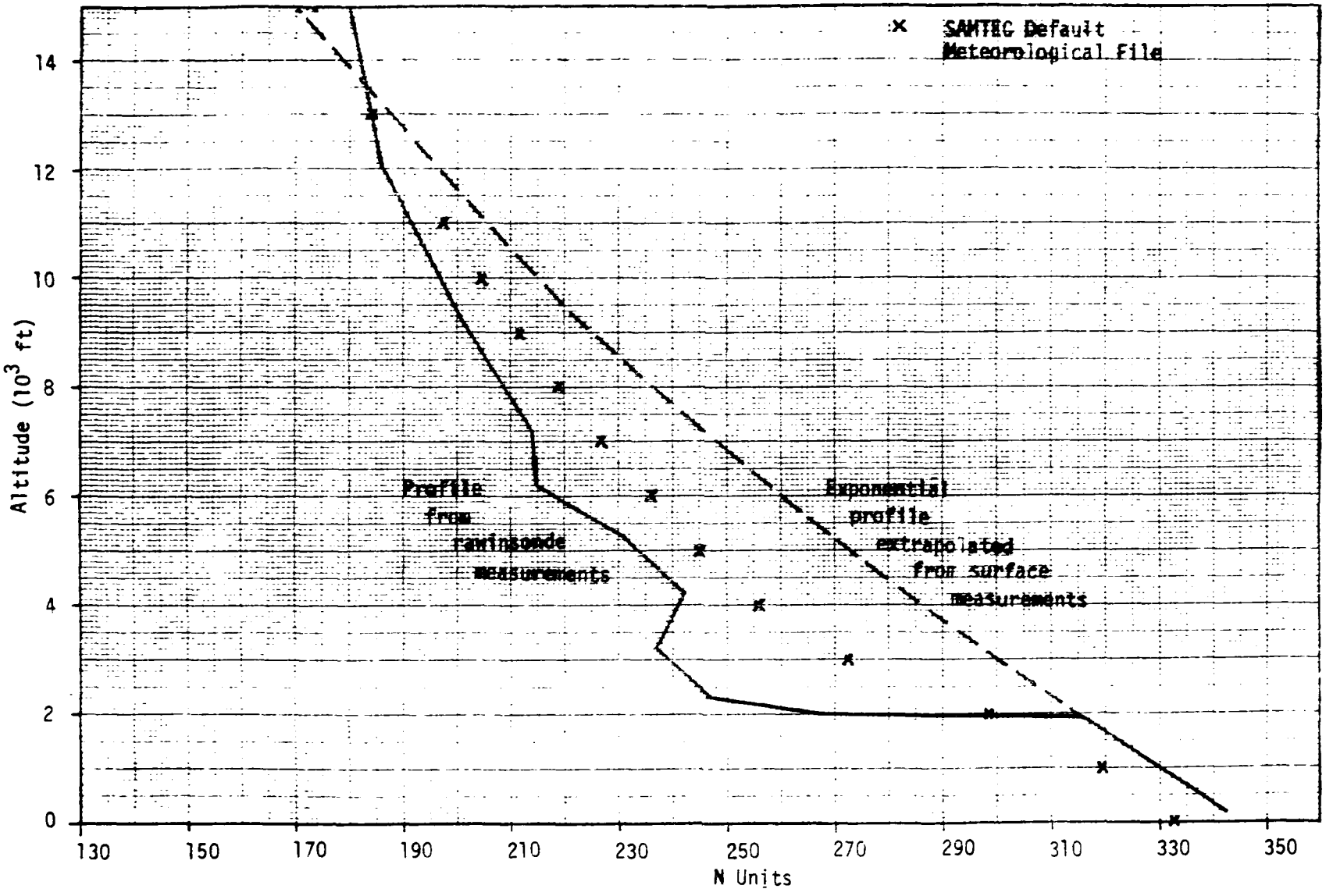

Figure 3.2 The refractivity profile obtained from rawinsonde measurements and selected model profiles (Pillar Point, Op. 6290, July 15, 1976)

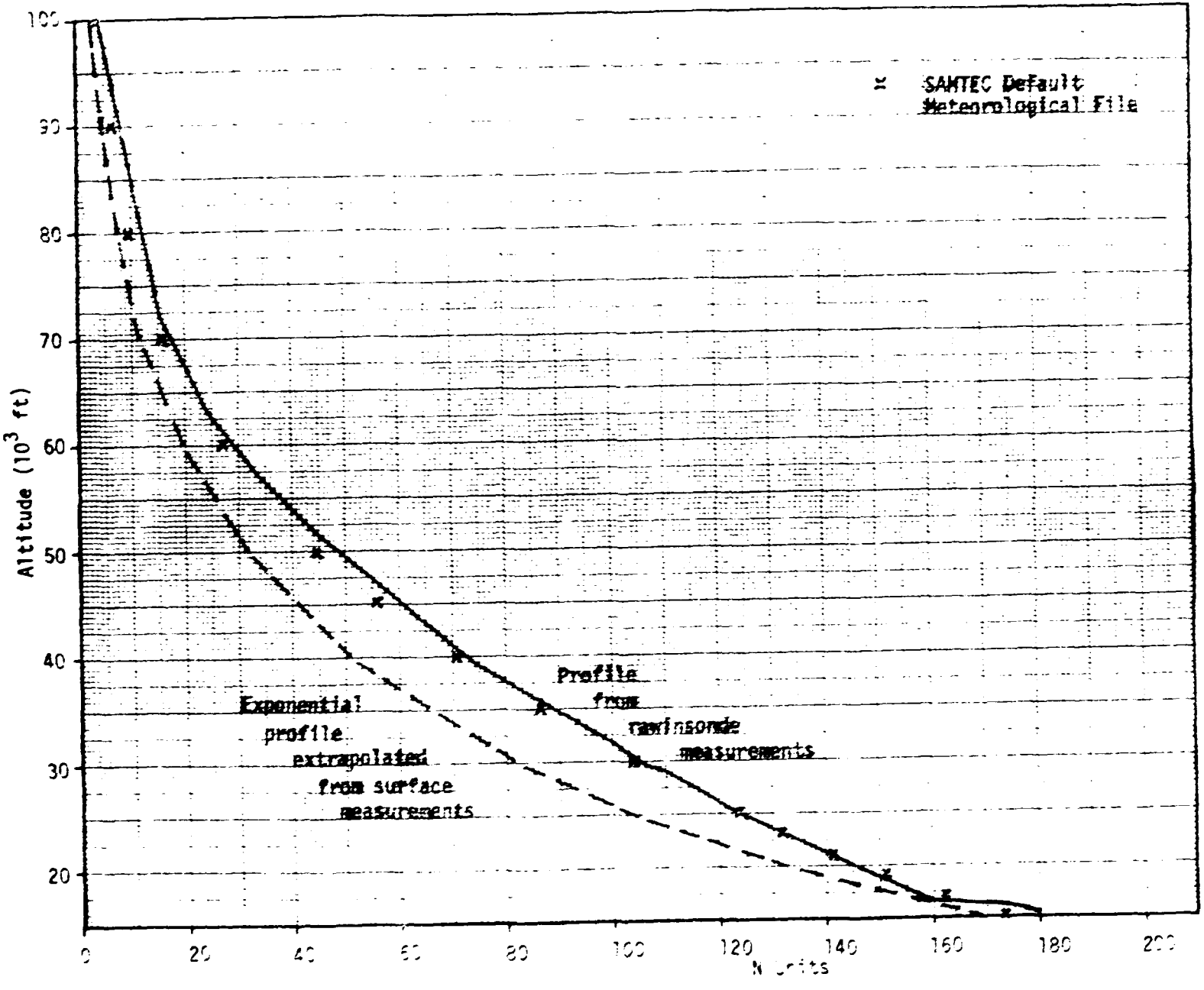

Figure 3.2 (Continued)

become larger than those of exponential profiles. The differences between them can be more than 20 N units. Above 100,000 ft, the two kinds of profiles both approach zero. Compared with the exponential profiles, the mean profile of SAMTEC Default Meteorological File is much closer to the measured profiles, except for the region below 15000 ft. In the region above 15,000 ft, the mean profile traces the measured profiles quite faithfully. (On an annual basis, the refractivity profile is seen to vary almost inmeasurably for altitudes greater than 25,000 feet.) On the other hand, the mean profile does not reveal any inversion layer.

The profiles obtained for Op 3445 are shown in Figures 3.3 and 3.4. Based on the limited data included in this report, the conditions in the winter are different from the conditions in the summer. First of all, there is no obvious inversion layer in these two winter profiles. Below 10,000 ft, the exponential profiles are closer to the measured profiles than the mean profile but above that the mean profile traces the measured profiles much more closely.

For the 4 cases observed, the closer proximity of the exponential model below 2K feet for summer and below 10K feet for winter were not nearly sufficient to offset the better fit of the mean model for the remainder of the profile.

3.2 Comparison of the Refraction Corrections

The refractivity profiles presented in the last section are input to the post-flight refraction correction module (REFRC). The calculated corrections on range and elevation angle based on the measured rawinsonde profiles are taken as the standards for comparison, from which the corresponding corrections based on the model profiles are subtracted. The differences are shown in Tables A.1 through A.4 in Appendix A. These differences can be considered as errors for each model if it is assumed that the rawinsonde-measured profiles and the corresponding corrections are the references. It is obvious that the errors for the exponential profile are larger than those for the mean profile. The percentages of the range and elevation angle errors in the total corrections are listed in Table 3.1. The percentage errors are always larger near the beginning and the end of the tracking than at the middle part because of the variation of the elevation angle.

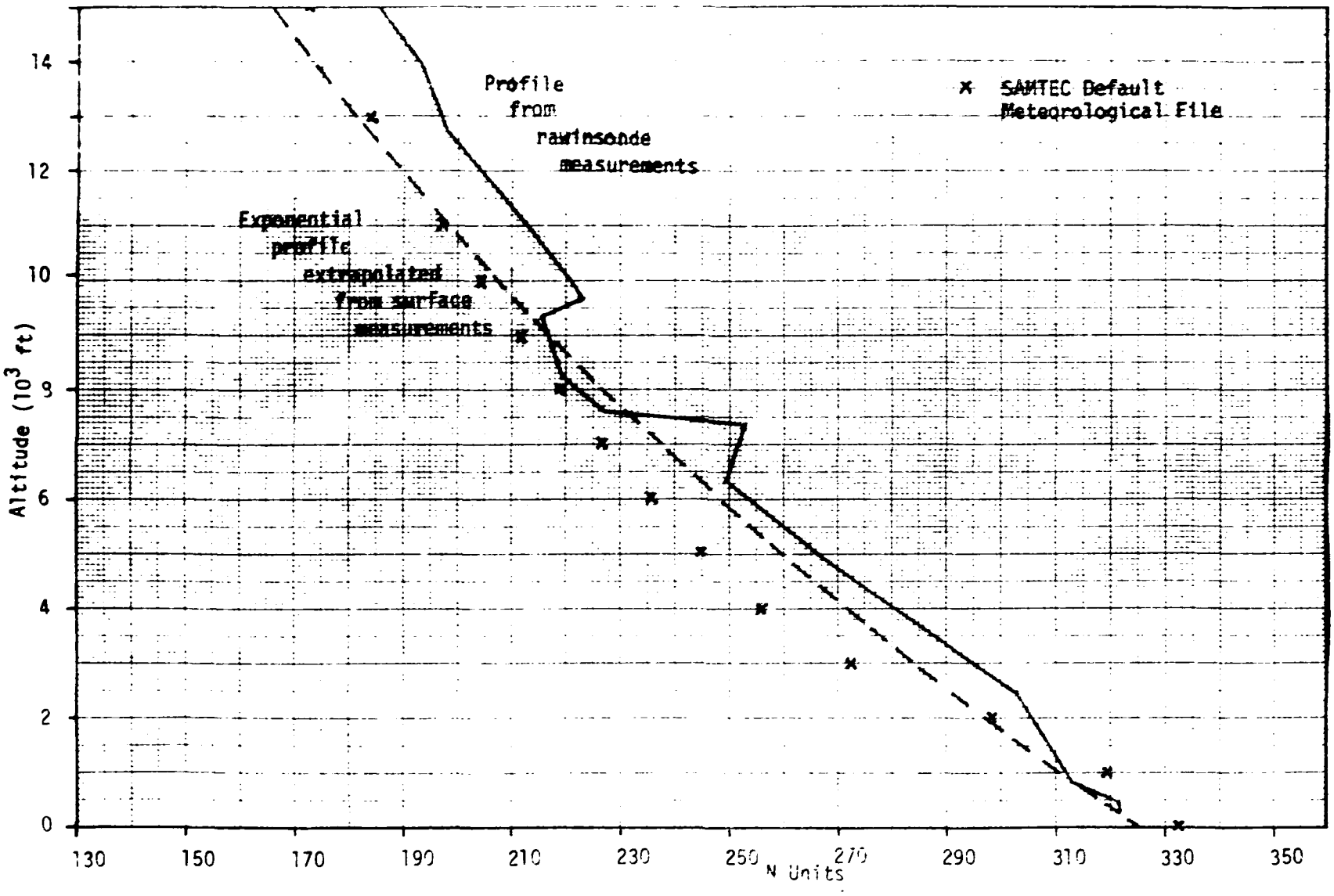

Figure 3.3 The refractivity profile obtained from rawinsonde measurements and selected model profiles (Vardenberg, Op. 3445, Jan. 21, 1977)

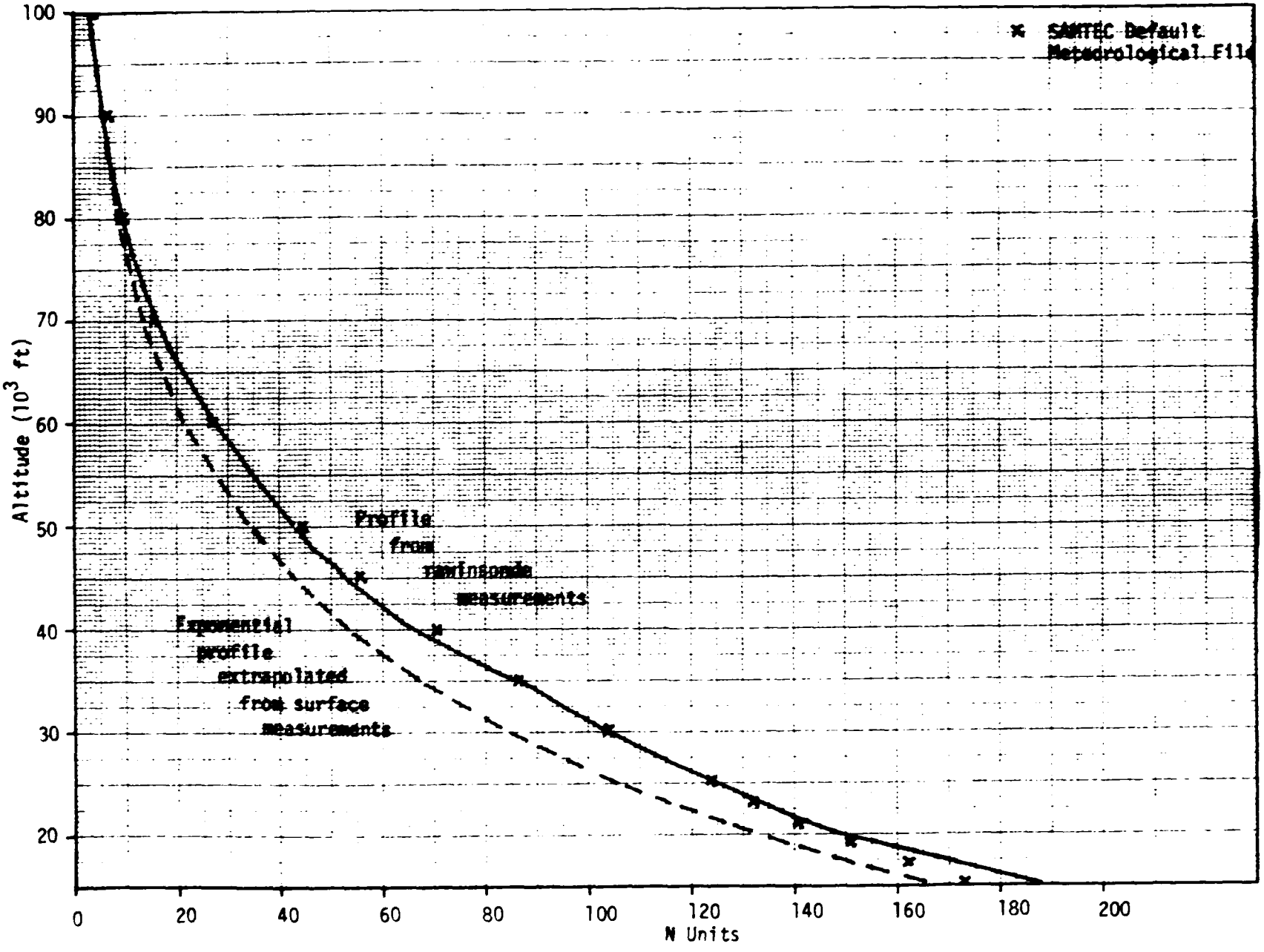

Figure 3.3 (Continued)

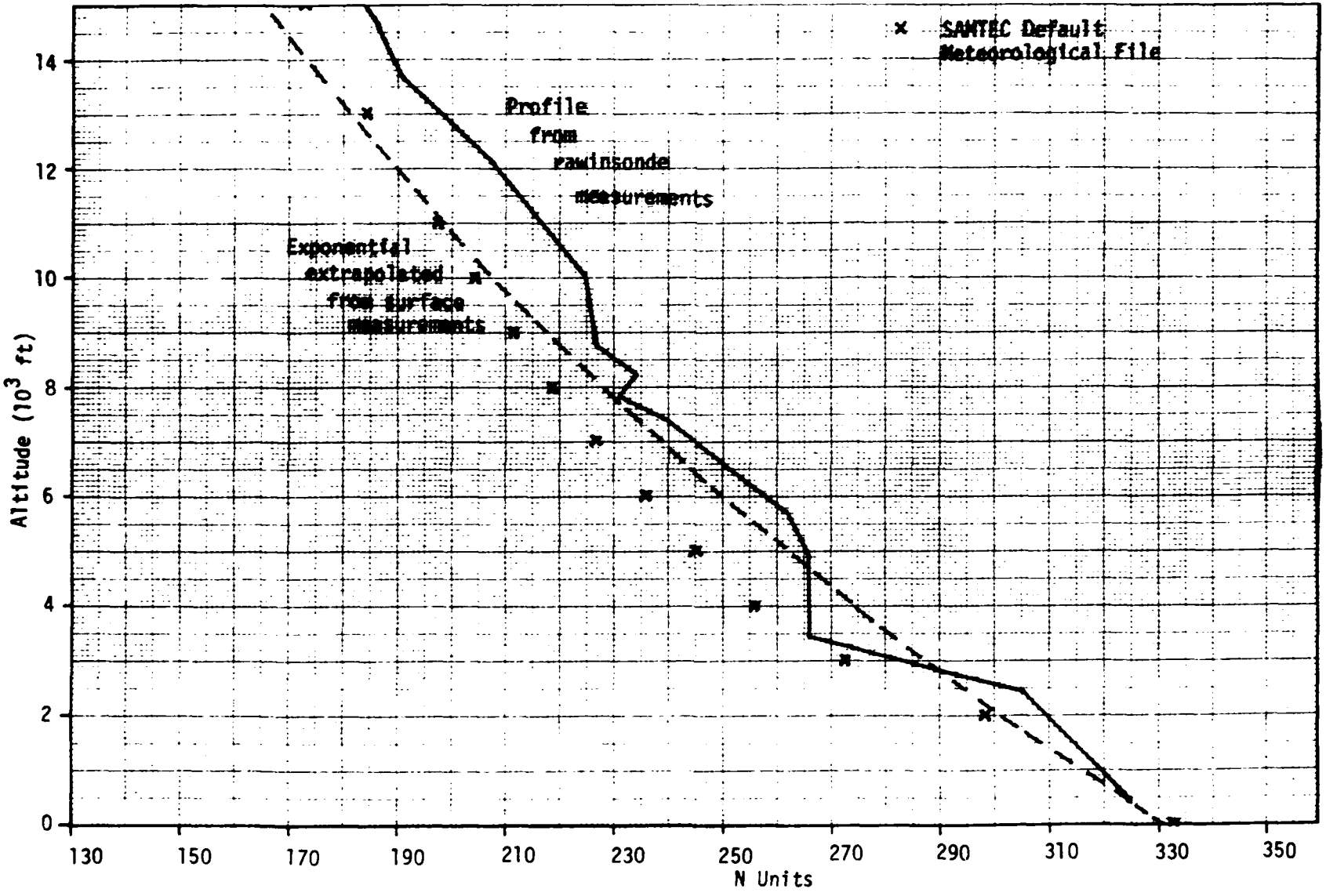

Figure 3.4 The refractivity profile obtained from rawinsonde measurements and selected model profiles (Pillar Point, Op. 3445, Jan. 21, 1977)

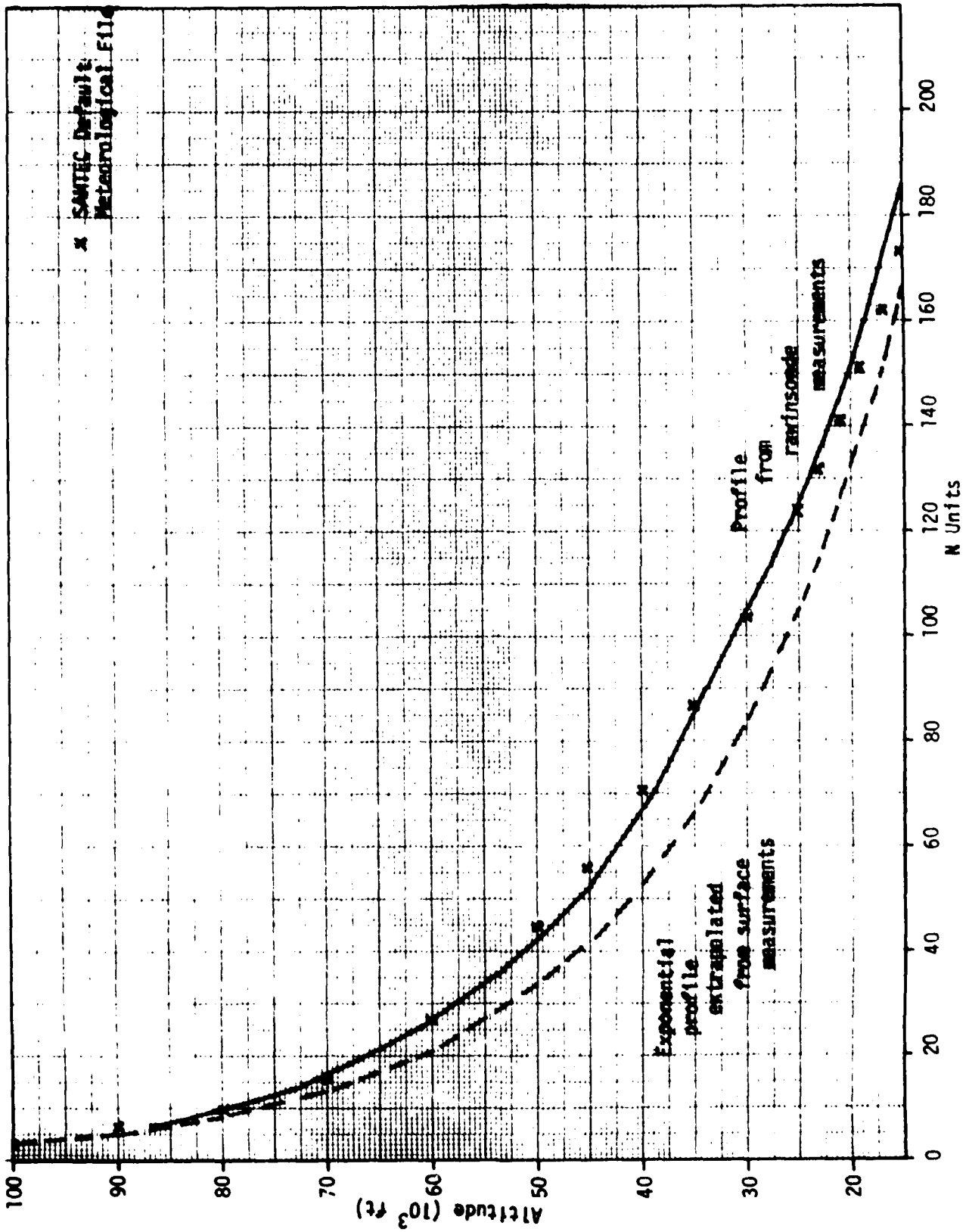

Figure 3.4 (Continued)

Table 3.1 The Percentage Errors in the Total Corrections

	July 15, 1976		January 21, 1976	
	Exponential profile	Mean profile	Exponential profile	Mean profile
Range Error	5-8%	0.2 - 1%	2-10%	2-3%
Elevation Angle Error	0.05-7%	0.01-4%	0.1-25%	0.1-25%

Table 3.2 Worst Case Refraction Correction Errors

	July 15, 1976		January 21, 1976	
	Exponential profile	Mean profile	Exponential profile	Mean profile
Range Error (ft)				
2° min. elev.	6.63	0.64	13.25	4.20
5° min. elev.	5.78	0.44	7.65	2.22
Elevation Angle Error (mils)				
2° min. elev.	.1883	.0345	.1473	.1483
5° min. elev.	.1883	.0245	.0390	.1033

Table 3.2 exhibits the corresponding worst case errors in terms of range and elevation correction magnitudes for minimum elevation angles of 2° and 5° for the 4 cases observed.

3.3 Summary

From the above discussion, it is suggested that the mean profile should be used, rather than the exponential profile, at Vandenberg AFB and Pillar Point AFS in case no rawinsonde-measured profile is available. The mean profile used in this study is the grand annual mean. It is also suggested that for actual range applications the seasonal or monthly mean profiles be obtained and tabulated in the SAMTEC Default Meteorology File.

4.0 ERRORS IN REFRACTION CORRECTIONS BASED ON MEASURED RAWINSONDE DATA

The errors in the refraction corrections can be considered as originating from the following sources:

(1) Errors in the collected rawinsonde data

  (a) sensor error

  (b) calibration error

  (c) stripchart reading error

(2) Errors introduced in processing the rawinsonde data to generate refractivity profile

  (a) error in converting the atmospheric parameters into the N-unit refractivity value.

  (b) error in deriving the corresponding height

(3) Errors introduced in calculating the refraction corrections from the given refractivity profile

  (a) error due to interpolation between input data points of refractivity profile

  (b) error in earth model (earth radius and geopotential model)

(4) Errors due to the difference between the region of rawinsonde measurements and the true signal path.

The first two error sources result in the total error in the derived refractivity profile. The third error source combined with the error in the refractivity profile causes the error in refraction corrections. The fourth error source accounts for the differences between the true refractivity profile under measurement and the one actually encountered by the radar signal. It is dependent upon the meteorological conditions and the real tracking environment. The relations among the various error sources can be best illustrated as in Figure 4.1.

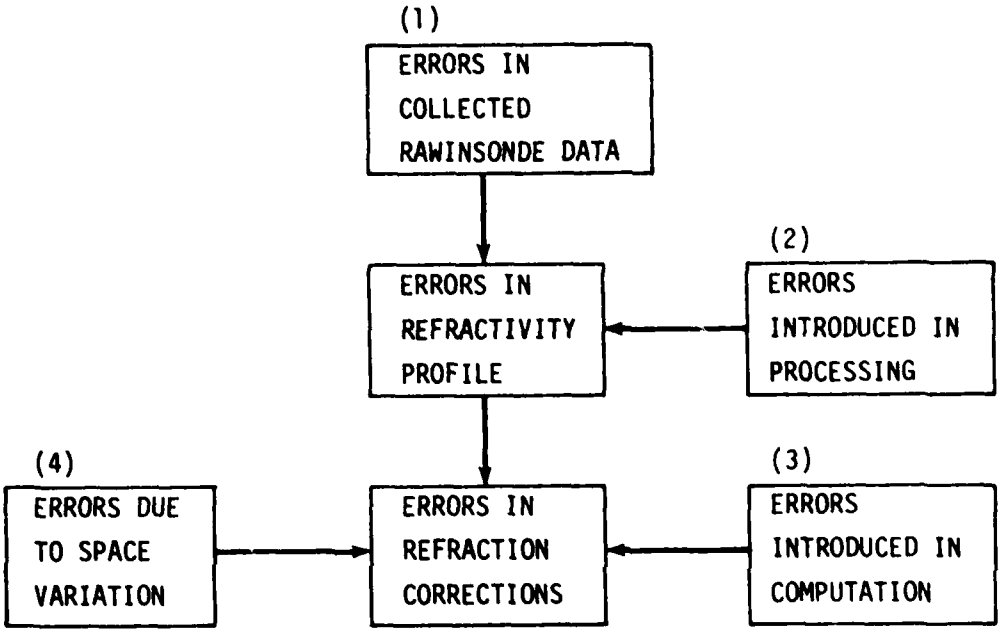

FIGURE 4.1 THE RELATIONSHIP AMONG VARIOUS ERROR SOURCES

4.1 Errors in the Collected Rawinsonde Data

The errors in the temperature, pressure, and relative humidity measured by rawinsonde are caused by the lag in sensor response, the bias in preflight calibration, and the error in stripchart recording/reading. According to the IRIG Document [4], these errors can be estimated by the so-called data reliability. By analyzing large numbers of rawinsonde measurements, the reliability of the data is established by estimating (1) the magnitude and type of systematic error, (2) the precision of the measuring process, and (3) the manner in which the individual measurements are distributed about the average. The term data reliability includes errors resulting from both human and instrumental sources. Where standards have been established, data reliability is a statement of accuracy. In general, however, the values of data reliability are statements of data precision to be expected from well maintained equipment, operated by competent individuals according to a well defined procedure.

The data reliabilities of temperature, pressure, and relative humidity measured by rawinsonde and ground instrument are listed in Table 4.1. These values are borrowed from the IRIG Document [4]. (A more recent IRIG document for meteorological data error estimates [14] was published after the computational work in this study was finished but the error values included therein are insignificantly different from those stated here.) Each of these values is a Root Mean Square deviation about a mean value which is the best estimate of the measure of the quantity. When applying these values to a particular rawinsonde launch, they represent the best estimates of systematic errors. The combination of these errors can result in systematic error in the refractivity profile and, in turn, systematic error in refraction corrections.

4.2 Errors in the Refractivity Profiles

4.2.1 Errors Propagated from Rawinsonde Data

The rawinsonde-generated refractivity profile used in the postflight refraction corrections consists of the discrete data points of the significant and 1000-foot levels. The error in the profile can be analyzed in two respects, the error in the calculated refractivity values and the error in the derived height of each data point.

Table 4.1 Data Reliability of Meteorological Parameters

Parameter and Instrument Types	Range of Values or Environment	Data Reliability*
Surface Measurements		
Temperature	-90°F to +145°F	0.5°F
Pressure (Aneroid Barometer)	840 to 1040 mb	0.3 mb
Relative Humidity (Wet/Dry Bulb)	Temp. above +32°F	3%
	Temp. below +32°F (5 to 100% RH)	6%
Upper Air Measurements		
Temperature	Surface to 20 km	1°C
	20 km to 30 km (-90°C to 60°C)	2.5°C
Pressure	10 to 50 mb	1.0%
	50 to 200 mb	0.6%
	200 to 500 mb	0.3%
	greater than 500 mb	0.2%
Relative Humidity	Temp. above 0°C	5%
	0°C to -20°C	10%
	-20°C to -40°C	20%
	Temp. below -40°C (5 to 99% RH)	unreliable

*Root Mean Square (RMS) deviations about a mean value which can be considered the best estimate of the measure of the quantity.

The error in the calculated refractivity values can be estimated by differentiating Equation (2.5). The result is given below,

$$\Delta N = A \cdot \Delta T + B \cdot \Delta E + C \cdot \Delta P \qquad (4.1)$$

where

$$A = \frac{-(77.6\ P - 11.0\ E)}{TK^2} - \frac{2 \times 374808\ E}{TK^3}$$

$$B = \frac{-11.0}{TK} + \frac{374808}{TK^2}$$

$$C = \frac{77.6}{TK}$$

$$\Delta E = \Delta(RH) \cdot 6.11 \cdot 10^X + RH \cdot 6.11 \cdot \mathrm{Log}_e(10) \cdot 10^X\ \Delta X$$

$$X = \frac{7.5\ T}{(237.3 + T)}$$

$$\Delta X = \frac{7.5\ \Delta T}{(237.3 + T)} - \frac{7.5\ T\ \Delta T}{(237.3 + T)^2}$$

where

P = total pressure (mb)

E = vapor pressure (mb)

T = temperature (°C)

TK = temperature (°K)

RH = relative humidity (%)

ΔP = error in the measured pressure (mb)

ΔT = error in the measured temperature (°C)

$\Delta(RH)$ = error in the measured relative humidity (%)

ΔE = error in the derived vapor pressure (mb)

ΔN = error in the derived refractivity

The meteorological parameters measured by rawinsonde in supporting Op 6290 are listed in Tables B.1 and B.2 in Appendix B. Also tabulated are the corresponding data reliabilities. By applying the data from these tables to Equation (4.1), the errors in the refractivity values are generated and are also listed in the tables together with the refractivity values from the originally measured parameters.

The error contributions from the three parameter measurements (temperature, pressure, and relative humidity) are compared and are presented in Tables B.3 and B.4. Generally, the contribution from the error in relative humidity is the largest below 30,000 ft. The error in temperature has the second largest effect and the pressure-induced error has the smallest effect. These observations are true because among the coefficients in Equation (4.1) B is the largest, A is the second and C is the smallest for most of this altitude region. Above 30,000 ft, the humidity-induced error becomes less dominant while the temperature-induced and pressure-induced errors become more significant. It is also noted that A is always a negative number and both B and C are positive. The signs of ΔT, ΔE, and ΔP can be either plus or minus. For the largest possible value of ΔN, the sign chosen for ΔT should be opposite to the signs chosen for ΔE and ΔP. The values of ΔN listed in Tables 4.2 and 4.3 are the largest possible values.

The error in the derived height of each data point can be evaluated by using the following formulas,

$$\Delta Z = \frac{GRRA \cdot GARR}{(GRRA - HGT)^2} \Delta(HGT) \qquad (4.2)$$

$$\Delta(HGT) = \Delta(HGTP) + [HV\ TVB\ \mathrm{Log}_{10}\ e\ (\frac{P\ \Delta(PP) - PP\ \Delta P}{PP\ P}) + HV\ \mathrm{Log}_{10}\ \frac{PP}{P}\ \Delta(TVB)]$$

$$\Delta(TVB) = \frac{1}{2}\ [\Delta(TV) + \Delta(TVP)]$$

$$\Delta(TV) = \frac{(1 - 0.379\ \frac{E}{P})\ \Delta(TK) + 0.379\ TK\ (\frac{P\ \Delta E - E\ \Delta P}{P^2})}{(1-0.379\ \frac{E}{P})^2}$$

$$\Delta(TVP) = \frac{(1 - 0.379 \frac{EP}{PP}) \cdot \Delta(TKP) + 0.379\ TKP\ (\frac{PP \cdot \Delta(EP) - EP \cdot \Delta(PP)}{(PP)^2})}{(1 - 0.379 \frac{EP}{PP})^2}$$

where
- $\Delta(TK)$ = error in the measured temperature at current level (°K)
- ΔP = error in the measured pressure at current level (mb)
- ΔE = error in the derived vapor pressure at current level (mb)
- $\Delta(TKP)$ = error in the measured temperature at previous level (°K)
- $\Delta(PP)$ = error in the measured pressure at previous level (mb)
- $\Delta(EP)$ = error in the derived vapor pressure at previous level (mb)
- $\Delta(HGTP)$ = error in the geopotential height at previous level
- TKP = temperature at previous level (°K)
- PP = total pressure at previous level (mb)
- EP = vapor pressure at previous level (mb)
- e = the base of the natural logarithm

These equations have been obtained by differentiating the equations used for deriving height in Section 2.2. Some variables and constants in the above equations were also explained in that section.

The same values of the meteorological parameters and their data reliabilities which have been used to evaluate the errors in refractivity values are applied to the above equations in an attempt to estimate the magnitude of the propagated error in the derived height for each data point. It is noted that, unlike the independence of the errors in the calculated refractivity values for different data points, the error in the derived height at a level is an accumulation of the height errors from all the previous levels plus the error at the current level. Therefore, the magnitude of the height error is quite small near the ground level and becomes larger at higher levels. It is indicated by the calculated results that the propagated errors in the derived heights are less than 100 feet for the levels below 15,000 feet and are not more than 500 feet around the altitude of 100,000 feet.

4.2.2 Errors Introduced in Processing

The previous error computations provide estimates of the refractivity profile errors due to the errors in the rawinsonde measurements. Considering the total error in the refractivity profile, the errors associated with the mathematic models, which are used to convert the atmospheric parameters into the refractivity values and the geometric heights, should also be taken into account.

One of the formulas used for the computation of refractivity values is in the following form,

$$N = K_1 \frac{P_d}{T} + K_2 \frac{e}{T} + K_3 \frac{e}{T^2} \tag{4.3}$$

where

P_d = dry air pressure in mb
T = temperature in °K
e = vapor pressure in mb

This formula is in a form different from that given in Equation (2.5). The total pressure (sum of dry air pressure and vapor pressure) is used in the first term of Equation (2.5) whereas the dry air pressure is used in Equation (4.3). These two equations can yield close results for the computation of refractivity. The constants K_1, K_2, and K_3 in Equation (4.3) have the following values and errors [2]:

$K_1 = 77.60 \pm 0.013$ °K/mb
$K_2 = 71.6 \pm 8.5$ °K/mb
$K_3 = (3.747 \pm 0.031)\ 10^5$ °K/mb

The error in the refractivity which might be introduced by the errors in the constants can be evaluated by using the following equation,

$$\Delta N = \Delta K_1 \frac{P_d}{T} + \Delta K_2 \frac{e}{T} + \Delta K_3 \frac{e}{T^2} \tag{4.4}$$

where ΔK_1, ΔK_2, and ΔK_3 represent the errors in the three constants.

Assuming a high-humidity condition with P_d = 1000 mb, T = 288°K, and e = 12 mb on the ground, the error in refractivity is approximately 1 N unit. The major contribution to this error comes from the vapor pressure terms. If the air is completely dry, the error in refractivity is only 0.05 N unit. At higher altitudes, both P_d and e drops down and the value of ΔN becomes smaller than that on the ground.

The height of each data point is calculated by using the barometric equation which is based on the assumption of hydrostatic equilibrium. Hydrostatic equilibrium is a balance between all forces along the vertical. The actual acceleration of a parcel along the vertical is ordinarily so small in comparison with gravity that the basic assumption of hydrostatic equilibrium is sufficiently accurate for all practical purposes. One potential error source in the mathematic model for height calculation is from the error in the gravity constant which is used in converting geopotential height to geometric height. This error can be evaluated by using the following formula,

$$\Delta Z = \frac{HGT}{GRRA - HGT}\ \Delta(GARR) - \frac{GARR * HGT}{(GRRA - HGT)^2}\ \Delta(GRRA) \qquad (4.5)$$

where
- ΔZ = error in the derived geometric height
- HGT = geopotential height
- GRRA = the combined gravitational and radius of the earth factor for station latitude
- GARR = the radius of the earth factor for station latitude
- $\Delta(GARR)$ = error in GARR
- $\Delta(GRRA)$ = error in GRRA

This equation is derived from Equation (2.4). It is estimated by using the above equation that the errors in the geometric height caused by an error of 0.125 percent of the gravity constant (approximately a quarter of the gravitational variation from the equator to the pole) are less than 60 feet for altitudes lower than 30,000 feet and less than 200 feet for altitudes lower than 100,000 ft.

4.2.3 Refractivity Profiles with Errors

The refractivity errors estimated in Sections 4.2.1 and 4.2.2 are added to give the total error in refractivity value for each data point of the significant levels. The same is also done for the height errors estimated in these two sections to give the total error in height. The resultant refractivity error and height error can be either positive or negative. Considering all the possible combinations of the signs of these two types of errors, there are totally four erroneous data points associated with each originally derived data point. The two erroneous data points which are resulted from pairing the same signs of the refractivity and height errors have the largest deviations from the original data point. These erroneous data points are shown with the original data point for each significant level in Figures 4.2 and 4.3, for the profiles measured over Vandenberg and Pillar Point in supporting Op 6290.

A large number of refractivity profiles can be formed from these erroneous data points by connecting them in different ways. Four of them can be considered as representative cases: the two bounding profiles which are formed by connecting all the erroneous data points on one side of the original profile and the two zigzag profiles which are formed by connecting alternatively the erroneous data points on the two sides. The two zigzag profiles are shown together with the original profile in Figures 4.2 and 4.3.

4.3 Errors in the Refraction Corrections

4.3.1 Errors Propagated from the Measured Profile

When a refractivity profile is used for computing refraction corrections, the errors in the profile are propagated into the corrections. In order to evaluate the propagated errors in the corrections the four erroneous profiles discussed in Section 4.2.3 and the original profile are applied to the REFRC module. The corrections computed from the original profile are taken as the standards for comparison. The corrections derived from each of the four erroneous profiles are subtracted from the standards. The differences can be considered as errors for each case.

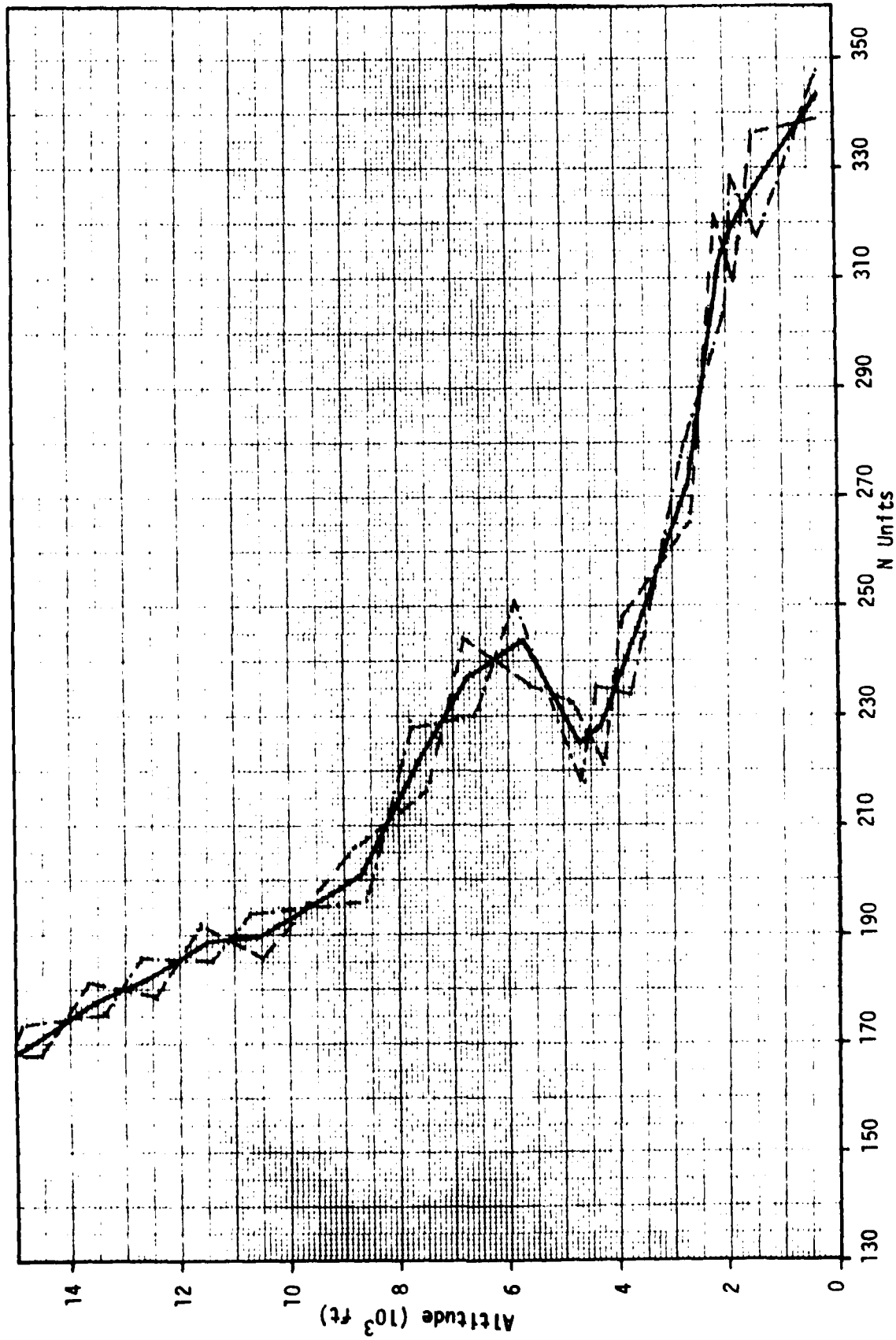

Figure 4.2 Errors in refractivity profile obtained from rawinsonde measurements (Vandenberg, Op. 6290, July 15, 1976)

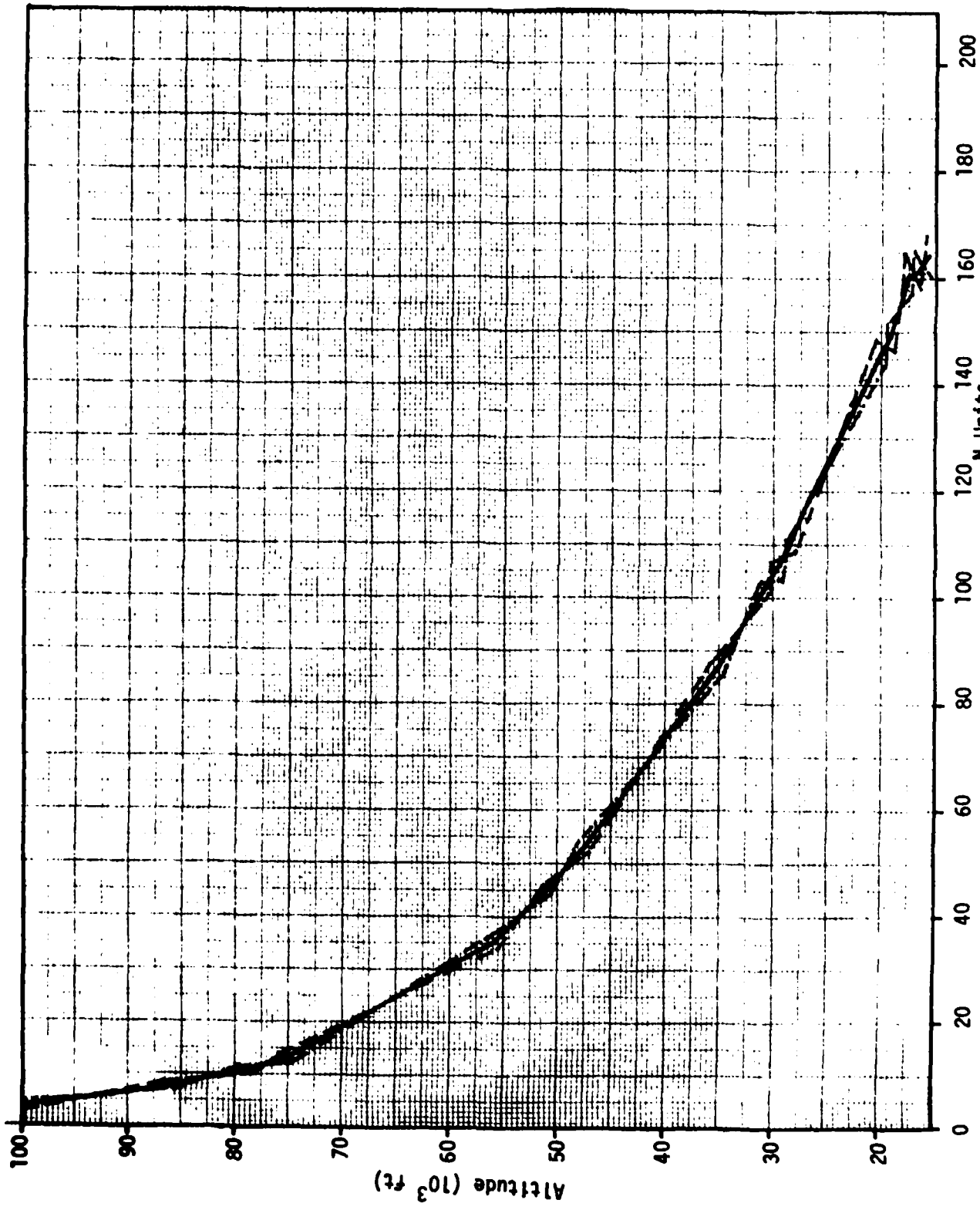

Figure 4.2 (Continued)

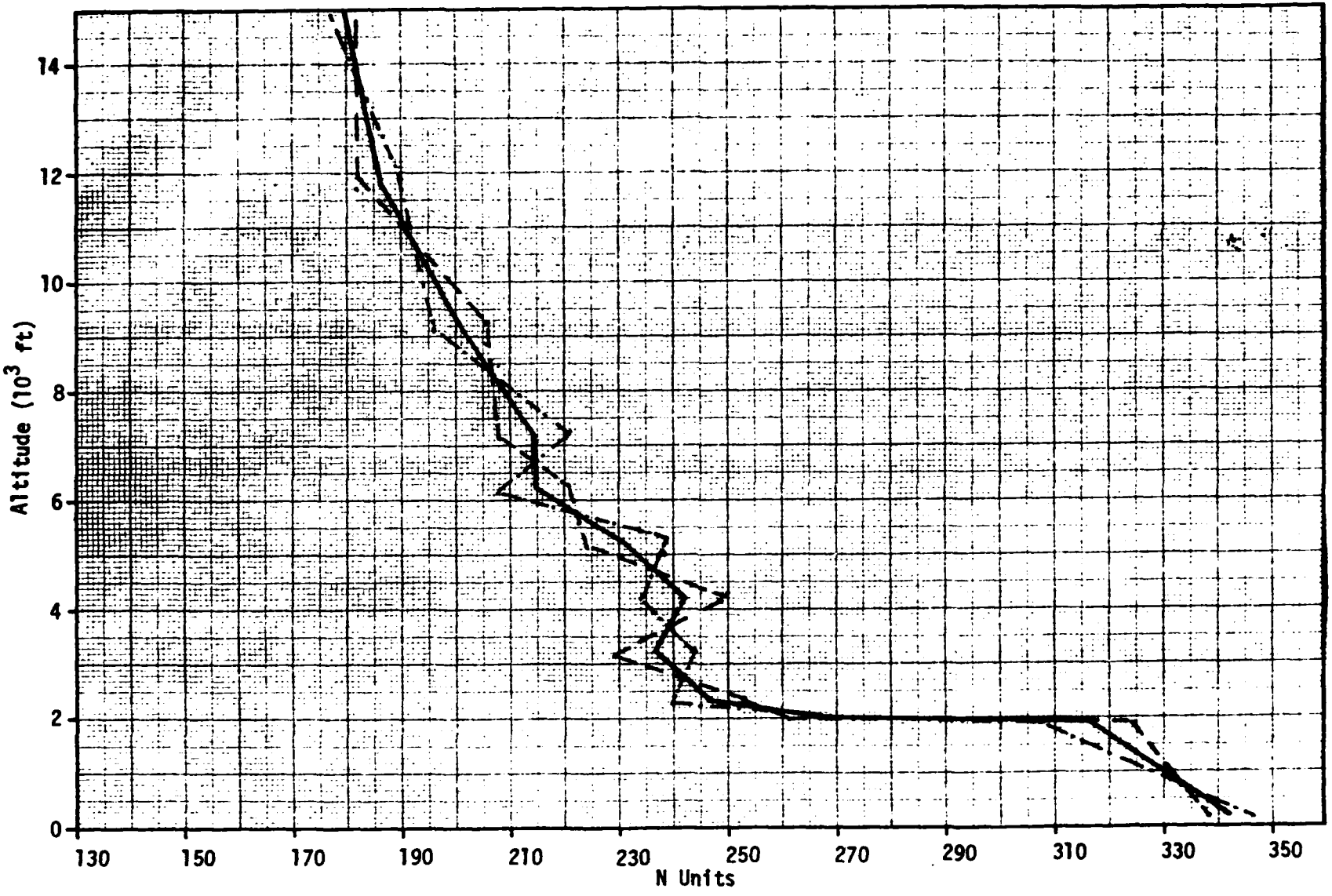

Figure 4.3 Errors in refractivity profile obtained from rawinsonde measurements (Pillar Point, Op. 6290, July 15, 1976)

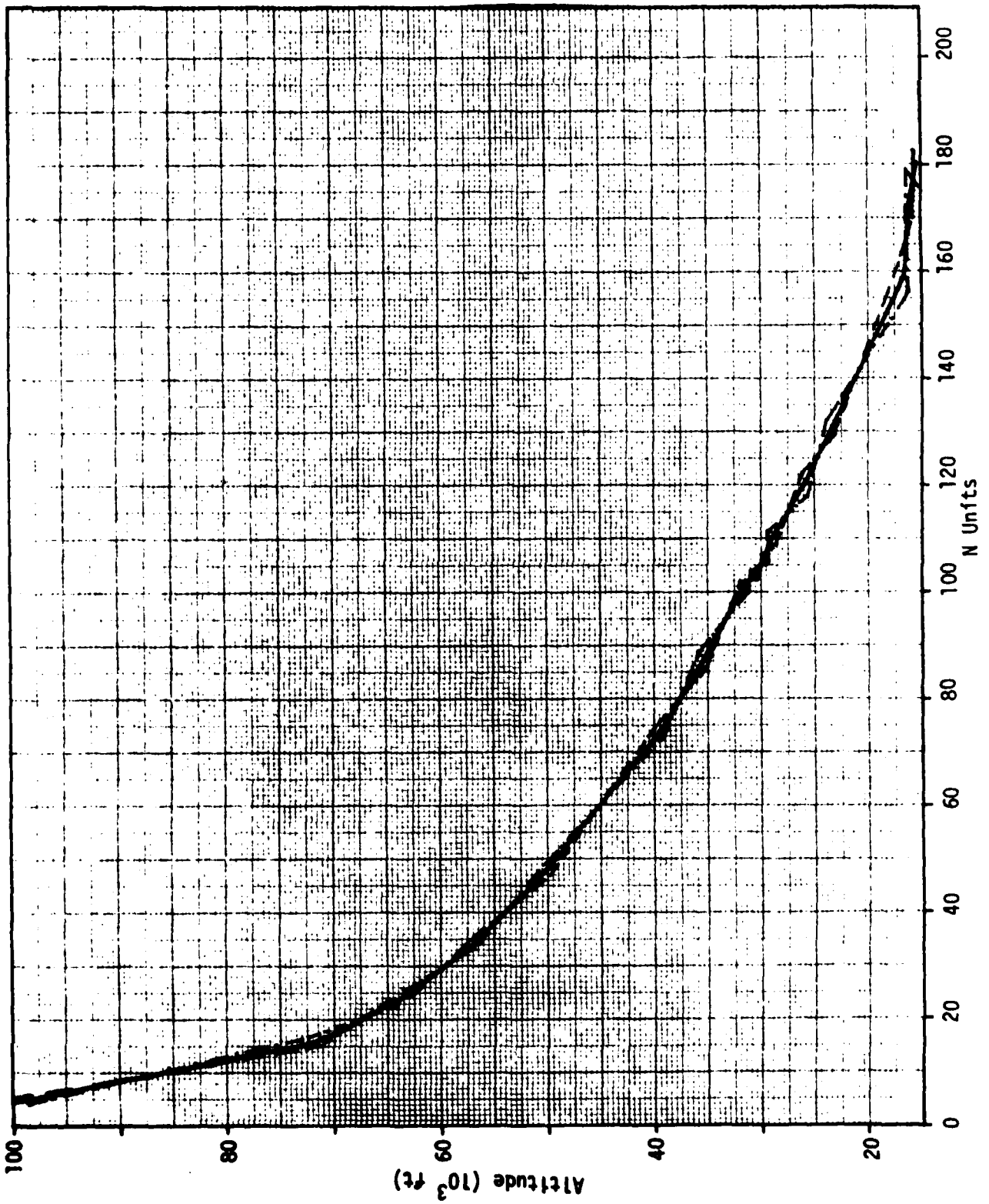

Figure 4.3 (Continued)

The refraction correction errors on range and elevation angle for Radar 213002 in supporting Op 6290 are plotted versus flight time in Figures 4.4 and 4.5 and are also listed in Table C.1 in Appendix C. For comparison the difference between the measured profile corrections and CRPL model corrections are also presented (denoted DR_{01} and DE_{01}) in Figures 4.4 and 4.5. The errors shown in these figures are either positive or negative. The positive error means an error due to undercorrection whereas the minus error means an error caused by overcorrection. The corrected elevation angles are marked on the time axis. The angle is small at the beginning of the tracking and increases with the flight time. At approximately 200 seconds, it starts to become smaller and decrease through the rest of the part of tracking. Both the range and elevation angle errors are larger at the beginning and the end of the tracking because of the small elevation angles. The two range error curves (DR_{02} and DR_{03}) based on the two bounding erroneous profiles are quite symmetric to each other. The other two range error curves (DR_{04} and DR_{05}) derived from the two zigzag erroneous profiles are also in symmetry. Similar symmetric conditions hold true for the four curves of elevation angle error. The absolute magnitudes of the range errors due to the bounding profiles are larger than those due to the zigzag profiles. Because the refraction correction on range is dependent upon the integrated refractivity along the signal path, the range error is accumulated along the path in the case of the bounding profile while the error is compensated at the different part of the path for the zigzag profile. The absolute magnitudes of the elevation angle errors due to the zigzag profiles, on the other hand, are larger than those due to the bounding profile. This is because the amount of refraction correction on elevation angle is determined by the refractivity and its gradient along the signal path, and the zigzag profile has steeper gradients than the smoother bounding profile. However, the bounding profiles represent the true erroneous profile more realistically than the zigzag profiles because the errors in the refractivity gradients are normally of the systematic type.

The estimated refraction correction errors for Radar 023003 in supporting Op 6290 and for Radars 213002 and 023003 in supporting Op 3445 are listed in Tables C.3 through C.4 in Appendix C. They have the same characteristics as described above.

In cases considered, the errors in range corrections are approximately 2 to 3 percent of the corrections. The errors in elevation angle corrections are less than or around 1 percent.

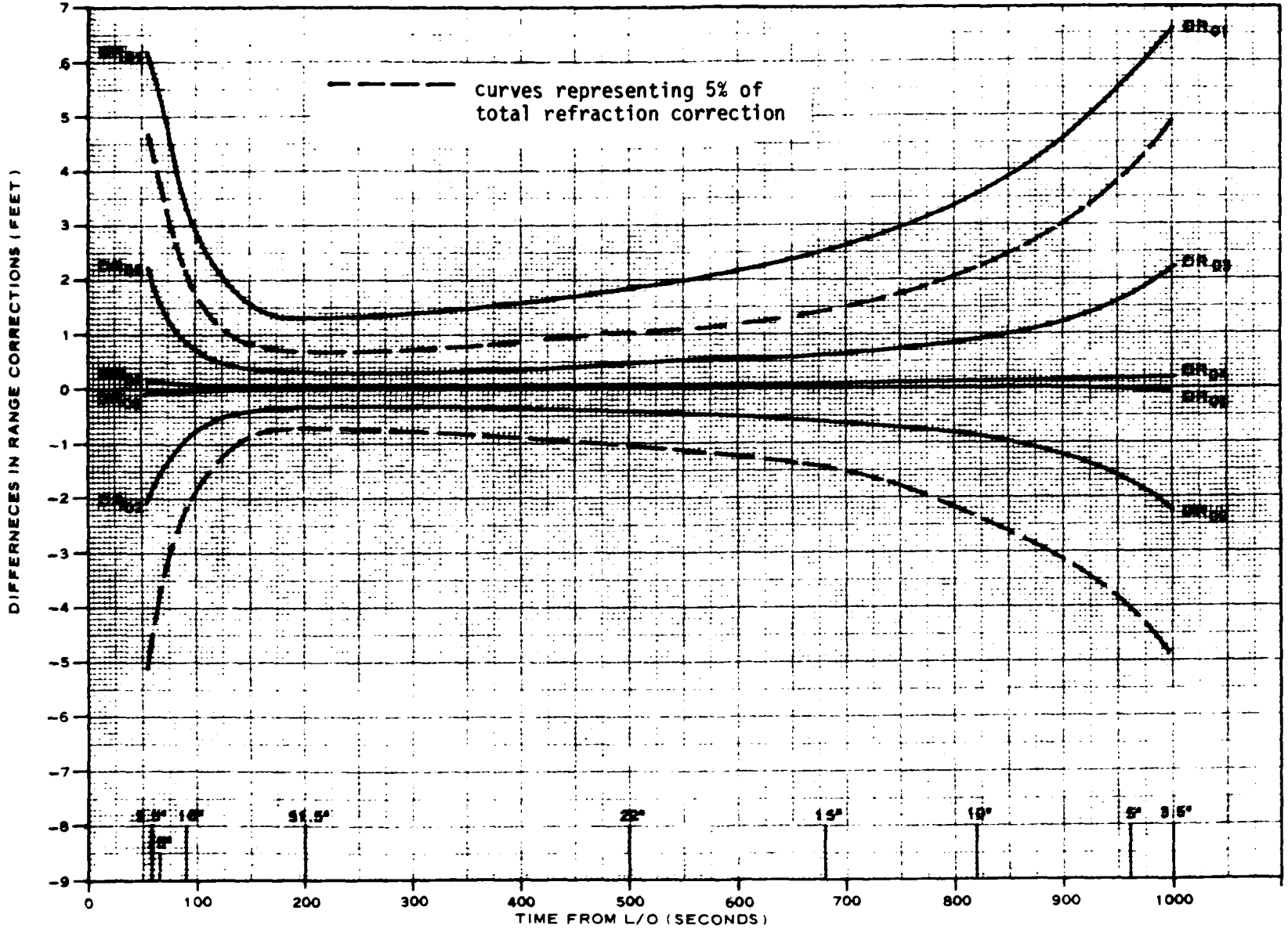

FIGURE 4.4 THE ERRORS OF REFRACTION CORRECTION FOR RANGE

(OP 6290, RADAR 213002)

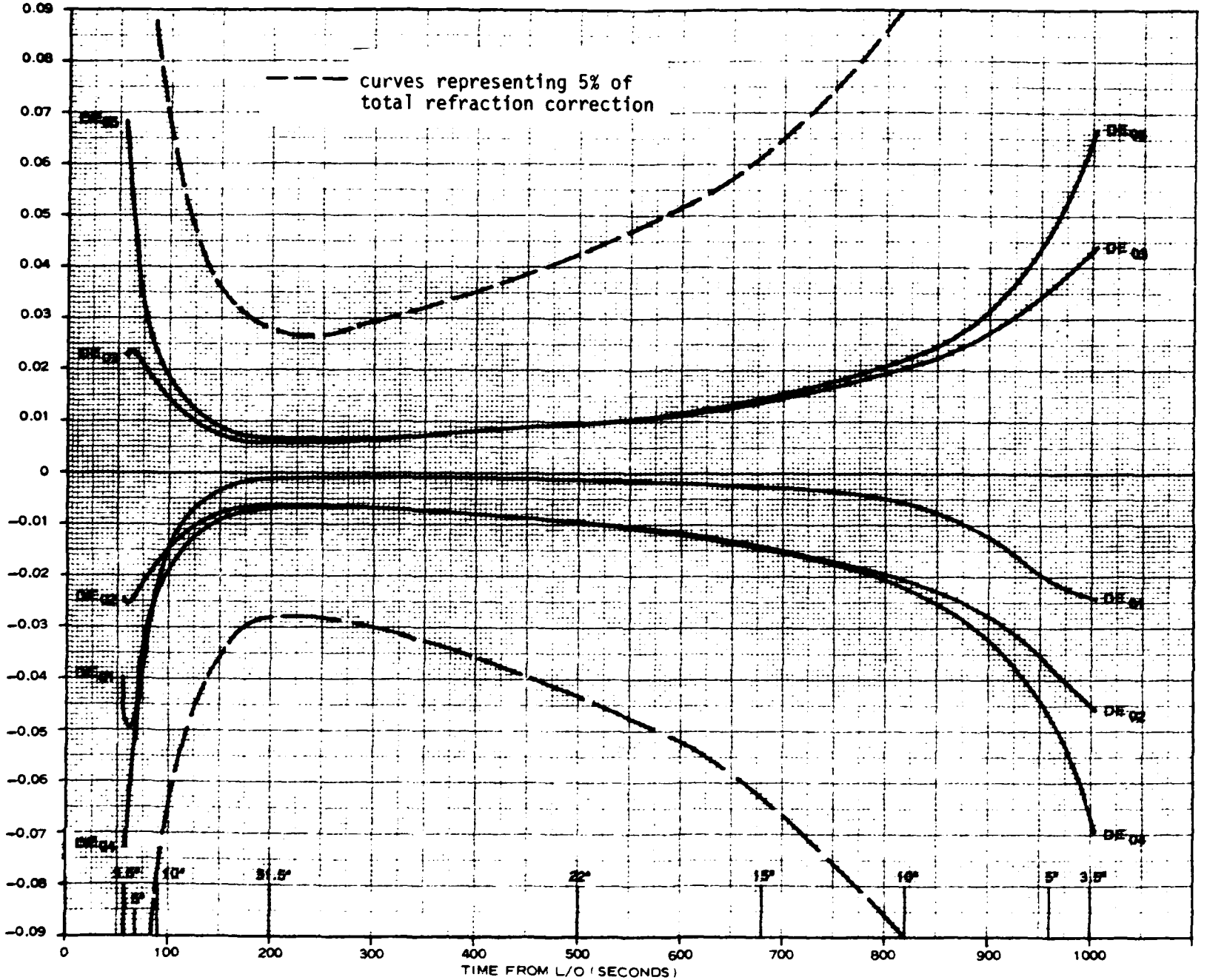

FIGURE 4.5 THE ERRORS OF REFRACTION CORRECTION FOR ELEVATION ANGLE (OP 6290, RADAR 213002)

4.3.2 Errors Introduced in Computation

The mathematic model of the REFRC module was originally developed at PMTC. This model has been widely accepted by many other ranges. In this refraction study, no effort was devoted to mathematically checking the accuracy of the REFRC module. This refraction correction model, known as REFRAC before, has been compared with others [6, 7, and 8]. Some of the results of the comparisons are listed in Table 4.2. It can be seen from this table that for elevation angles larger than 3.5 degrees the differences between the corrections generated by the REFRAC and others are less than 1 ft and 0.02 mil. (The angle difference of 0.08 mil is excluded because the model RECA is not considered to be valid for low elevation angles near 3.5 degrees.) However, these values do not represent the errors of this model. They merely supply some quantitative indication of the consistency between the REFRAC mathematic model and the other models. The assumption made in this study is that the range and angle errors, which can be introduced by the mathematic model, are less than the values of 1 ft and 0.02 mil for elevation angles larger than 3.5 degrees. They represent the percentage errors of less than 1 percent for range and less than 0.5 percent for elevation angle.

4.4 Errors Due to Space Variation

It has been realized that the atmosphere is not purely spherically stratified as assumed in the mathematic model of ray tracing technique. For the purpose of refraction correction, the refractivity profile should be measured along the true signal path. However, the rawinsonde can seldom follow the signal path to make the measurements. Therefore, the refractivity profile measured by rawinsonde and used for refraction corrections could be different from the real profile experienced by the signal on its path of propagation. The estimation of the magnitudes of the errors in refraction corrections due to this difference has been one of the major concerns in discussing the accuracy of refraction corrections based on rawinsonde data.

A more complete answer to this needs statistical analysis based on long-term experiment with proper instrumentation to observe the N-unit bias and variability for different height levels. This kind of data is not available

Table 4.2 Results of the Comparisons Made for Different Refraction Correction Programs*.

	Range	Elevation	Remarks
REFRAC - RECA (ETR) [6]	$\leq$ 0.6 ft	$\leq$ .08 mil	E $\geq$ 3.5°
REFRAC - MERS2 (ETR) [7]	$\leq$ 1.0 ft	$\leq$ .02 mil	E $\geq$ 3.5°
REFRAC - REEK (ETR) [8]	$\leq$ 0.25 ft	$\leq$ .02 mil	E $\geq$ 3.5°

* Based on same input profiles for the comparisons.

to the current study. The only piece of information which can be addressed for this aspect of study for the Vandenberg and Pillar Point areas is contained in a paper written by Gardner [5]. Several simultaneous observations using rawinsonde and airborne refractometer were conducted in 1970 and were reported in this paper. The rawinsondes were launched in their regular role in supporting missile launches and the rawinsonde drifted to the east due to prevailing winds while the airborne refractometer was coordinated to make simultaneous measurements along the signal path.

The refractivity profiles obtained from the rawinsonde and refractometer measurements were compared. The refraction corrections based on these profiles were also computed. The differences in range and elevation angle corrections are shown in Tables 4.3 and 4.4. The differences between the corrections based on the rawinsonde and refractometer profiles are very small compared with the total corrections. The difference in range corrections is less than 1 - 2 percent of the total range correction. Generally, the difference in elevation angle correction is less than 0.25 percent of the total correction. These differences are generally smaller than the errors in the range and elevation angle corrections computed in Section 4.3.

4.5 Permissible Refraction Correction Errors for SAMTEC Radars

The permissible refraction correction errors represent the amounts of residual errors which, after applying refraction corrections, can be allowed to exist in the data without having any significant effect on the data quality —— accuracy. The determination of these errors has to rely on the considerations of the error budget sources (Appendix D), and it is suggested that the permissible refraction correction errors in range and elevation angle should be 2 feet and 0.03 mil, respectively, for vehicle tracking at elevation angles larger than 5 degrees.

4.6 Summary

The contributions from the various refraction error sources to the total refraction correction errors are summarized in Table 4.5, as the percentages of the total corrections. These error percentages are established

Table 4.3 Differences in Refraction Corrections Versus Flight Time Vandenberg

		Rawinsonde Minus REFRACTOMETER	
Flight Time Sec	Corrected Elevation Deg	DE Mils	DR Feet
25	12.7	.018	0
50	38.3	.000	0
100	38.4	.000	0
200	27.4	.000	0
300	22.4	.000	0
400	18.3	.000	0
500	14.4	.000	0
600	10.6	.001	-1
700	6.9	.001	0
800	3.2	.007	0
850	1.4	.039	-1

DE = Refraction Correction Differences for Elevation Angle Between Rawinsonde Derived Corrections and Refractometer Derived Corrections

DR = Refraction Correction Differences for Slant Range Between Rawinsonde Derived Corrections and Refractometer Derived Corrections

Table 4.4 Differences in Refraction Corrections Versus Flight Time Pillar Point

Flight Time Sec	Corrected Elevation Deg	Rawinsonde Minus REFRACTOMETER DE Mils	DR Feet
50	1.9	.008	0
100	12.4	.000	0
200	28.9	.000	0
300	25.1	.000	0
400	20.6	.000	0
500	16.3	.000	0
600	12.2	.000	0
700	8.3	.000	0
800	4.5	.000	0
850	2.6	.000	0

Table 4.5 Estimated Percentages of Various Residual Refraction Correction Errors

	Range*	Elevation Angle*
Errors propagated from measured profile	2-3%	1%
Errors introduced in computation	< 1%	<0.5%
Errors due to space variation	<1-2%	<0.25%
Total Error	<4-6%	<1.75%

* Errors are expressed in percentages of total refraction corrections.

for the corrections at elevation angles larger than 3.5 degrees. The total error expected for range correction is less than four to six percent and that for elevation angle correction is less than three percent. The total errors in range (feet) and elevation angle (mils) for Operation 6290 are shown in Figure 4.6. The range error is within the permissible refraction correction error for the flight time from T+90 seconds to T+800 seconds (elevation angles above 10 degrees). The elevation angle error is smaller than the permissible error during the period from T+80 seconds to T+850 seconds (elevation angles above 8 degrees). It should be noticed, however, that these total errors represent the upper bound of possible refraction errors for Operation 6290. The BET residuals might not show trends in a shape like the total error curves as shown in Figure 4.6.

The most recent IRIG document for meteorological data error estimates [14] was published after the above computations were finished. The main difference in the errors estimated by the IRIG Document 110-71 [4] and the newer IRIG Document 110-77 [14] is the form in which the error varies with the measured quantity or the rawinsonde altitude. In the Document 110-71 the error estimates are in the form of step functions whereas the errors presented in the Document 110-77 vary linearly within each given range. It has been estimated that the gross effect of the differences in the estimated errors will result in no more than 0.5 percent reduction in the percentage value given in Table 4.5 for the range error propagated from measured profile and no more than 0.3 percent reduction in the value given for the propagated angle error if the error estimates in the newer document are to be used. As far as the final result is concerned, these differences are not significant at all.

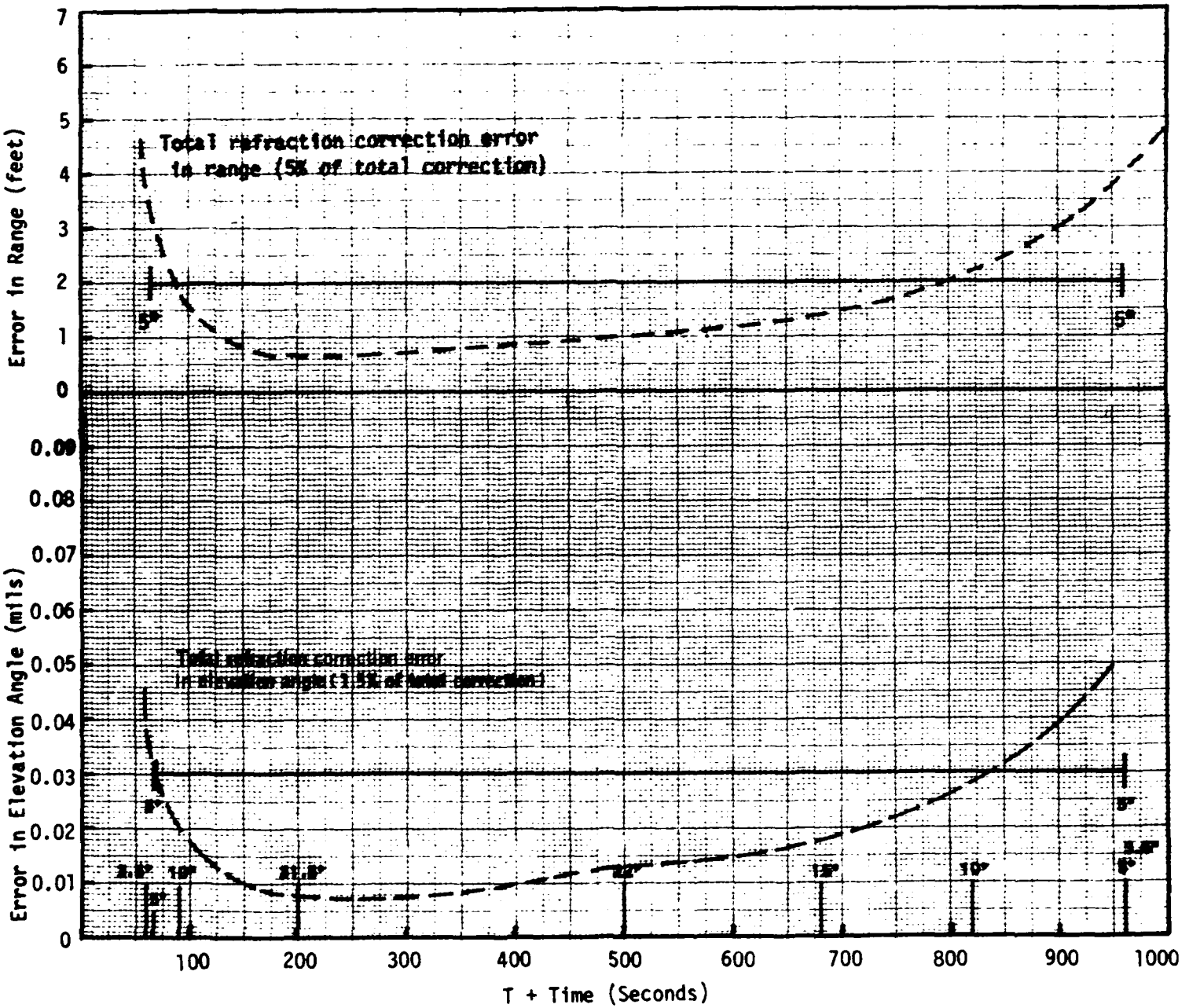

FIGURE 4.6 TOTAL REFRACTION CORRECTION ERRORS (Op 6290, Radar 213002)

5.0 MINIMUM HEIGHT REQUIRED FOR RAWINSONDE MEASUREMENTS

Generally the tropospheric refractivity profile follows an exponential decay with altitude. The mean value of refractivity at 100,000 ft is around 4 N Units over the Southern Californian Coastline. The refractivity becomes less than 1 N Unit above 120,000 ft. Because of less variability and also less significance of the profile above 100,000 ft, this altitude has been considered as a desired height to be reached by rawinsonde measurements. Generally a rawinsonde can make complete measurements starting from ground continuously to above 100,000 ft. Occasionally, some balloons might fail to reach this altitude. Questions have been raised concerning the minimum height required for rawinsonde measurements to adequately support range operations for refraction corrections. For a more definite answer to this question one has to give consideration to the following factors:

(1) the required accuracy of refraction corrections,

(2) the estimated errors in the regular refraction corrections based on complete rawinsonde measurements from ground to above 100,000 ft,

(3) the temporal variability of the refractivity as a function of height.

5.1 Errors Due to Incomplete Rawinsonde Measurements

In order to establish the requirement of the minimum height for rawinsonde measurements, the errors which can be introduced by missing different parts of the data below 100,000 ft should first be estimated. Then these estimated errors can be compared with the required accuracy of refraction corrections and the errors which were identified in Section 4.0.

The refractivity profiles obtained at Vandenberg AFB and Pillar Point AFS for Op 6290 can be considered "complete" because the rawinsondes launched to support this operation reached 100,000 ft and there is no missing data below this altitude. In order to investigate the residual refraction correction errors in different cases of incomplete rawinsonde measurements, which could be generated from the current procedure of postflight metric data reduction (MDR), the heights of 15,000 ft, 30,000 ft, and 60,000 ft

have been chosen separately as the "cutoff" heights for the rawinsonde measurements. In each case the data points of the originally measured profile are discarded above the cutoff height. The incomplete profile were sent to the MDR. The refraction corrections for range, elevation angle, and range rate were calculated, according to the current procedure. These refraction corrections are subtracted from the corresponding corrections based on the original complete profile. The differences are listed in Tables E.1 and E.2. The complete profile is assumed to represent the true profile and the differences listed in these two tables are treated as errors.

Large errors are shown for the cases with cutoff heights at 15,000 ft and 30,000 ft. Especially in the first case, the errors are even larger than the differences which can be expected between the corrections based on the originally measured profile and the exponential model profile shown in Section 3.0. Such large errors are caused by the linear interpolation made in the post-flight REFRC module for refractivity profile between the last measured data point and the data point with zero N unit assigned at 100,000 ft. Overall, a refractivity profile follows more closely to an exponential model than to a linear function. This linear interpolation causes overcorrection for range data and undercorrection for elevation angle data. The errors in the third case with cutoff height at 60,000 ft are much smaller than those in the first two cases because of the narrower missing data gap. Because the linear interpolation model is used, it is not acceptable to input two widely separated refractivity data points to the postflight refraction correction module.

The occurrence of large errors in the above cases does not indicate the existence of any mathematical problem in using linear interpolation in the REFRC module. Instead, it simply implies that the current procedure used to apply the REFRC module has to be modified in order to handle the cases of incomplete rawinsonde measurements correctly. One step should be included in the procedure. That is, additional data points should be filled in the large data gap of the incomplete rawinsonde measurements before the computer run of the REFRC module. It has been suggested [9] that the additional data points can be obtained from the exponential fitting between the last measured data point and the data point with 4 N unit assigned at 100,000 ft or from

the long-term mean refractivity profile. The mean profile might be a better choice because it is closer to the local true condition.

In order to see how much improvement can be obtained by filling the data gap in the suggested manner, two additional test runs were made. The first one has a cutoff height of 30,000 ft on the original profile and the mean profile of the SAMTEC Default Meteorological File is fitted above 30,000 ft up to 120,000 ft. The difference between the corrections based on this profile and those based on the original complete profile are also shown in Tables E.1 and E.2. It is indicated that the errors for both range and elevation angle are much reduced compared with the errors obtained for the profile with the same cutoff height but without filling the data gap. The second test run has a cutoff height of 15,000 ft on the original profile. Again the mean profile of the SAMTEC Default File is applied to the missing part of the data above 30,000 ft. The gap between 15,000 and 30,000 ft is filled by the exponential model fitted through the last measured data point and the Default data point at 30,000 ft. The refraction corrections calculated with this profile are subtracted from the corrections based on the original complete profile. The results are shown in Tables E.1 and E.2. Tremendous reduction of errors has also been obtained by filling the missing data in this way.

The range errors of the last two cases in Tables E.1 and E.2 are less than 2.5 percent of the range corrections. The elevation angle errors are less than 0.5 percent of the elevation angle corrections. These errors are smaller than the total refraction correction errors discussed in Section 4.6. They should be additive to the total errors to give an overall upper bound of the refraction correction errors. The results of the addition of the errors are shown in Figure 5.1, for the case with a cutoff height at 30,000 ft for Operation 6290. It is indicated by this figure that the range error due to cutoff at 30,000 ft will introduce only a small amount of additional error to total correction and the elevation angle error due to cutoff at the same altitude will result in insignificant increase of total correction error. Further improvement may be achieved by using the seasonal or monthly mean profile instead of the grand annual mean profile. Much more accurate results can also be expected if the previous or the following range-support or synoptic launch can provide the missing part of the data for the profile of interest.

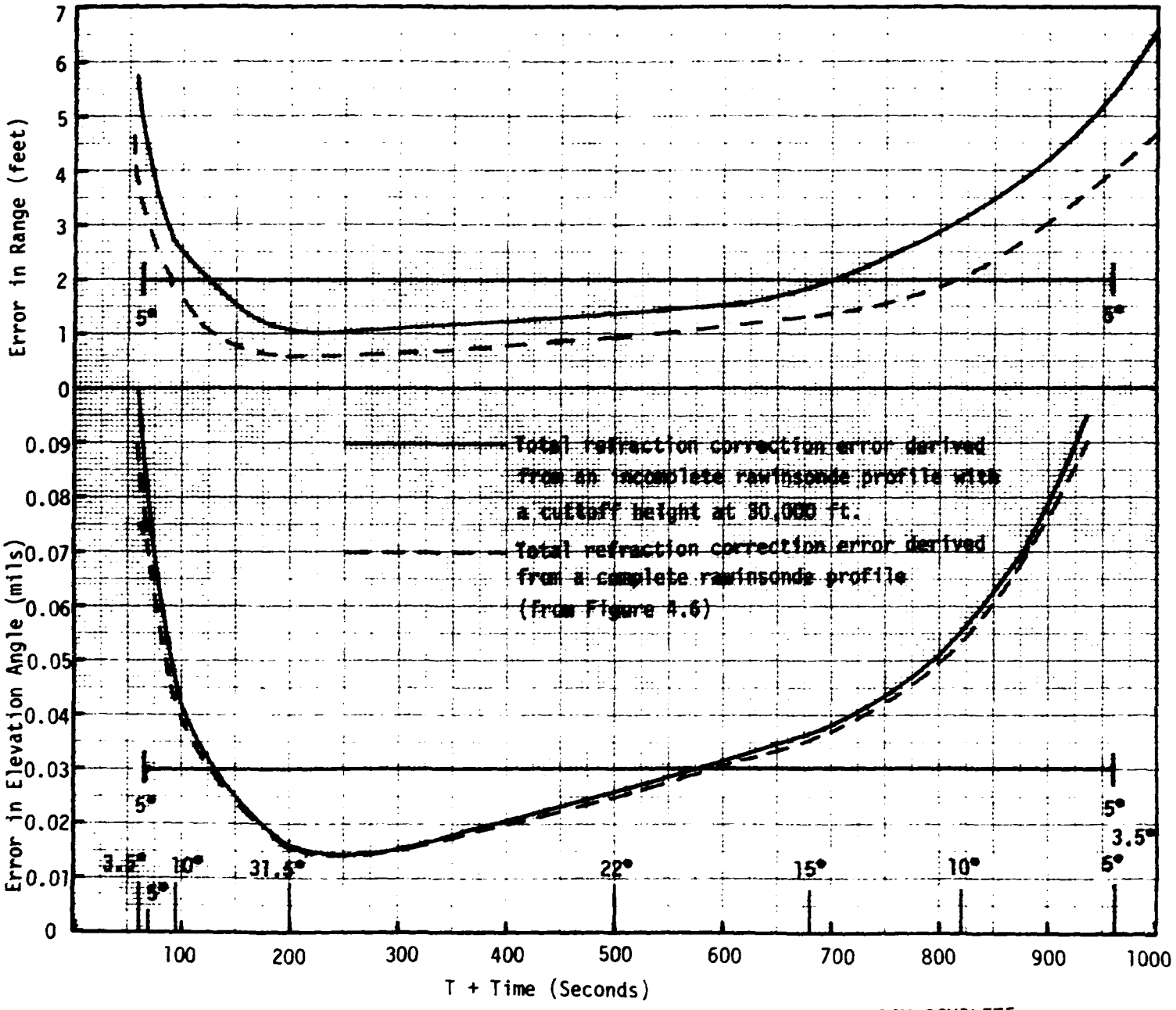

FIGURE 5.1 COMPARISON OF TOTAL REFRACTION CORRECTION ERRORS DERIVED FROM COMPLETE AND INCOMPLETE RAWINSONDE PROFILES (Op 6290, Radar 213002)

5.2 Temporal Variations of Refractivity Profiles

Before any conclusion can be drawn on the study of the minimum required height, there is one more thing which has to be checked. That is the diurnal temporal variation of the higher part of the refractivity profile. It is important to look into this because the results obtained above are based upon several measurements which constitute a very small sample and the confidence of any conclusion can only be established by combining the calculated results with a more general study of the temporal variability of the upper part of the refractivity profiles.

The temporal variation of the refractivity profiles can be best investigated by comparing the data collected by consecutive rawinsonde launches from the same site. Some of this kind of measurements have been performed at Vandenberg AFB [10]. The refractivity profiles are plotted in Figures 5.2 and 5.3, one for summer and one for winter study. It can be seen from these figures that the refractivity profiles do not show very significant diurnal variations for altitudes above 30,000 ft. The largest variation of refractivity above this height is not more than three N units. Most of time, the variations shown in the figures are in the order of the error which could be expected for regular rawinsonde measurements in this altitude region. The main reasons why the variations of the refractivity profiles above 30,000 feet are much smaller than those below this altitude can be explained by the following way. The most variable parameter in determining the refractivity values is the water vapor pressure because the relative humidity can vary from zero to 100 percent and below 30,000 ft the air can hold much more water. However, for the altitudes above 30,000 ft there is not much moisture, even for 100 percent relative humidity. The values of refractivity above this height are almost completely determined by the pressure and the temperature, which do not have any significant diurnal or daily variations above this altitude. There could be some seasonal variations for these two parameters due to the upward or downward shift of the tropopause.

As a matter of fact, the pressure and temperature measurements are the only valid measurements which can be performed by rawinsonde sensors above 30,000 ft. Since the temperature usually starts to drop below -40°C in the vicinity of this height, the relative humidity sensor does not function reliably and no valid humidity measurement can be provided.

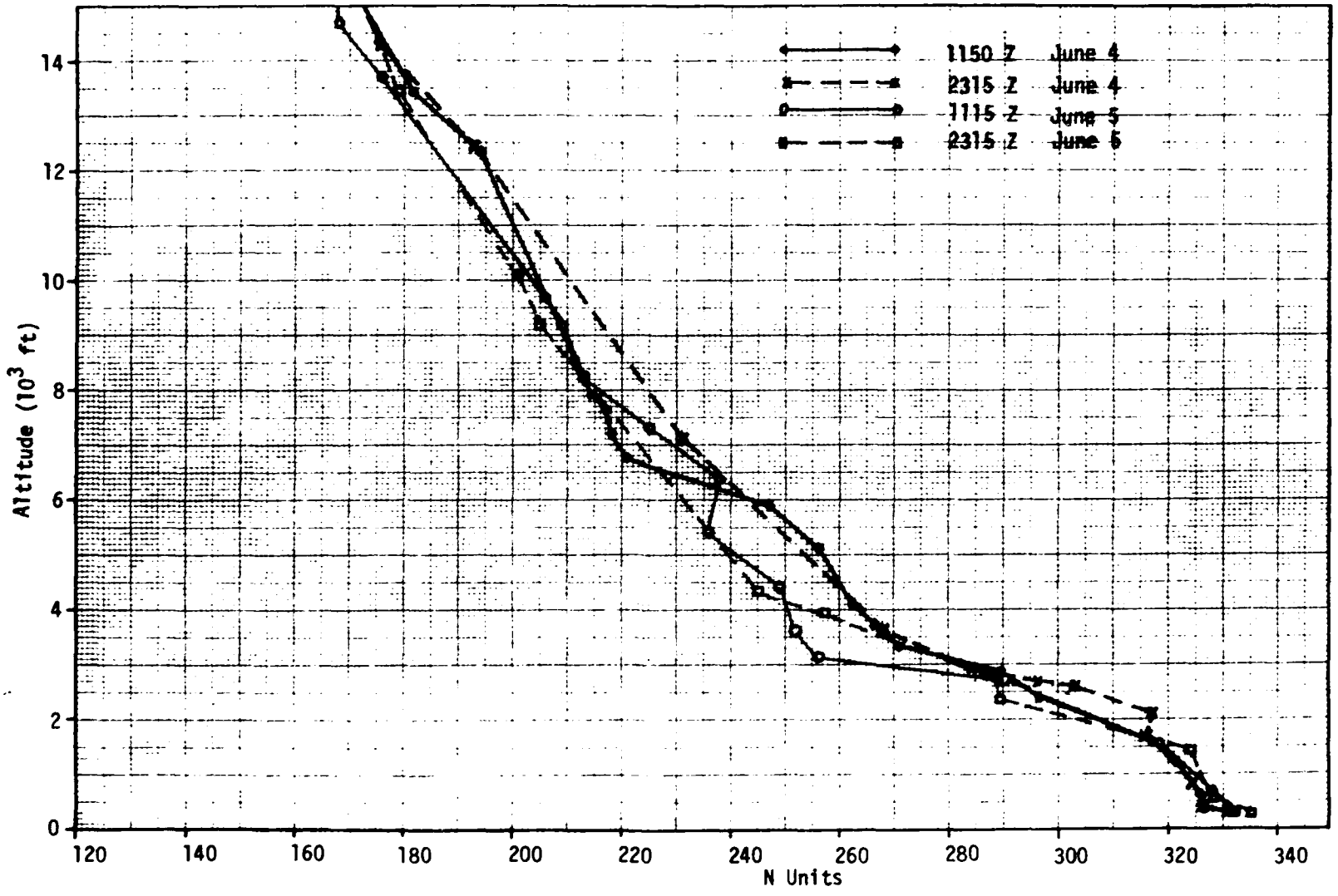

Figure 5.2 Refractivity profiles measured by rawinsondes launched at Vandenberg in summer

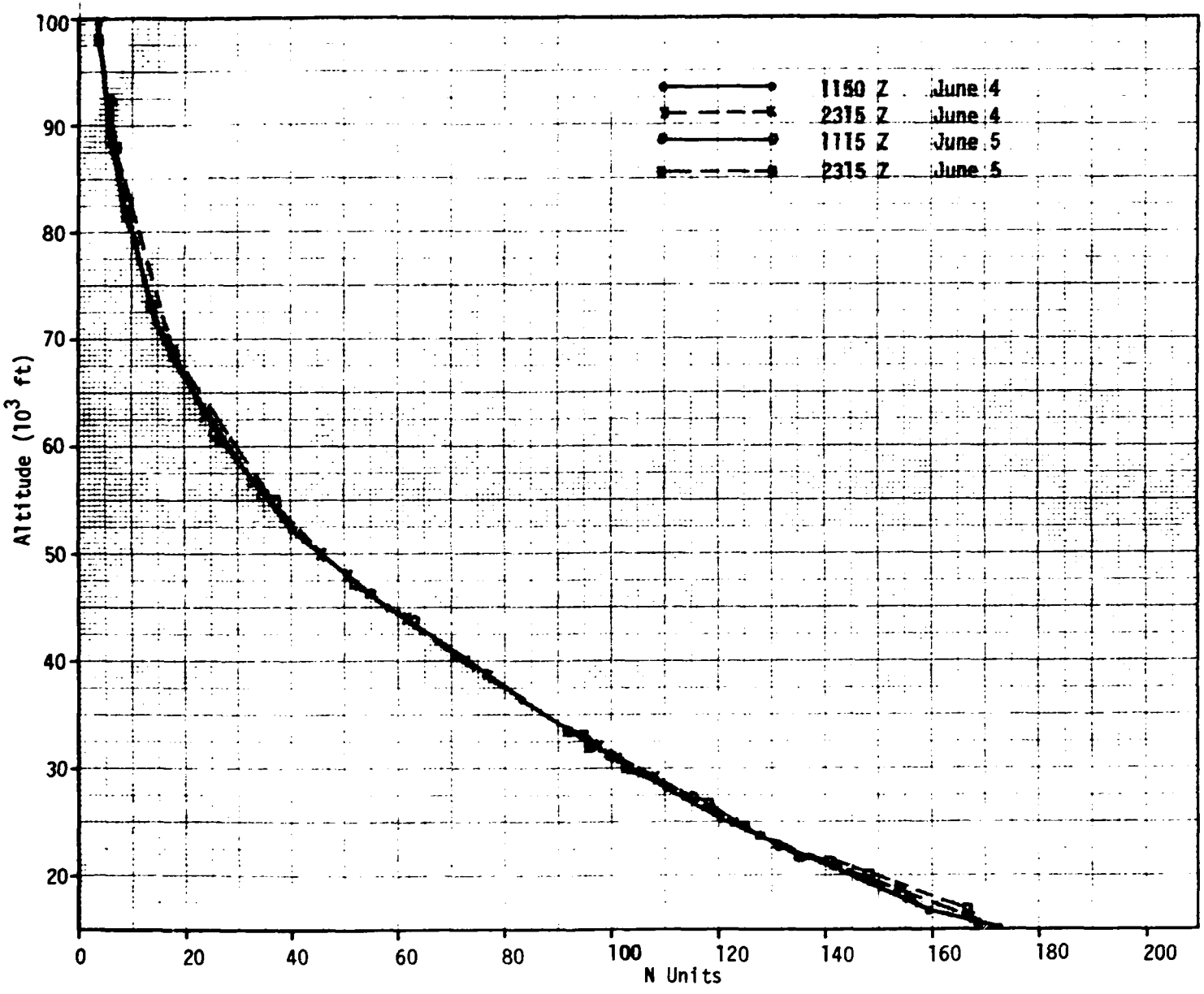

Figure 5.2 (Continued)

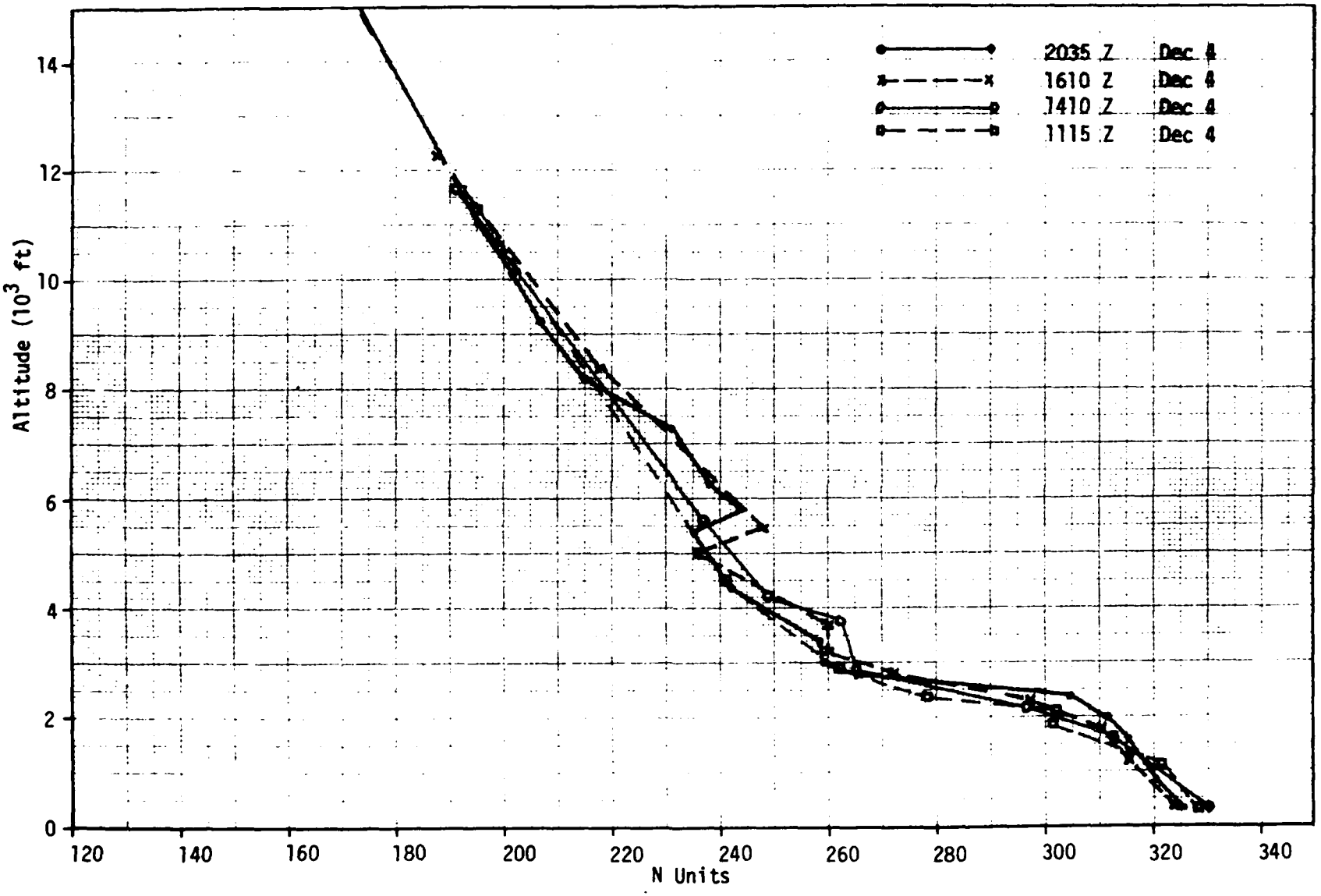

Figure 5.3 Refractivity profiles measured by rawinsondes launched at Vandenberg in winter

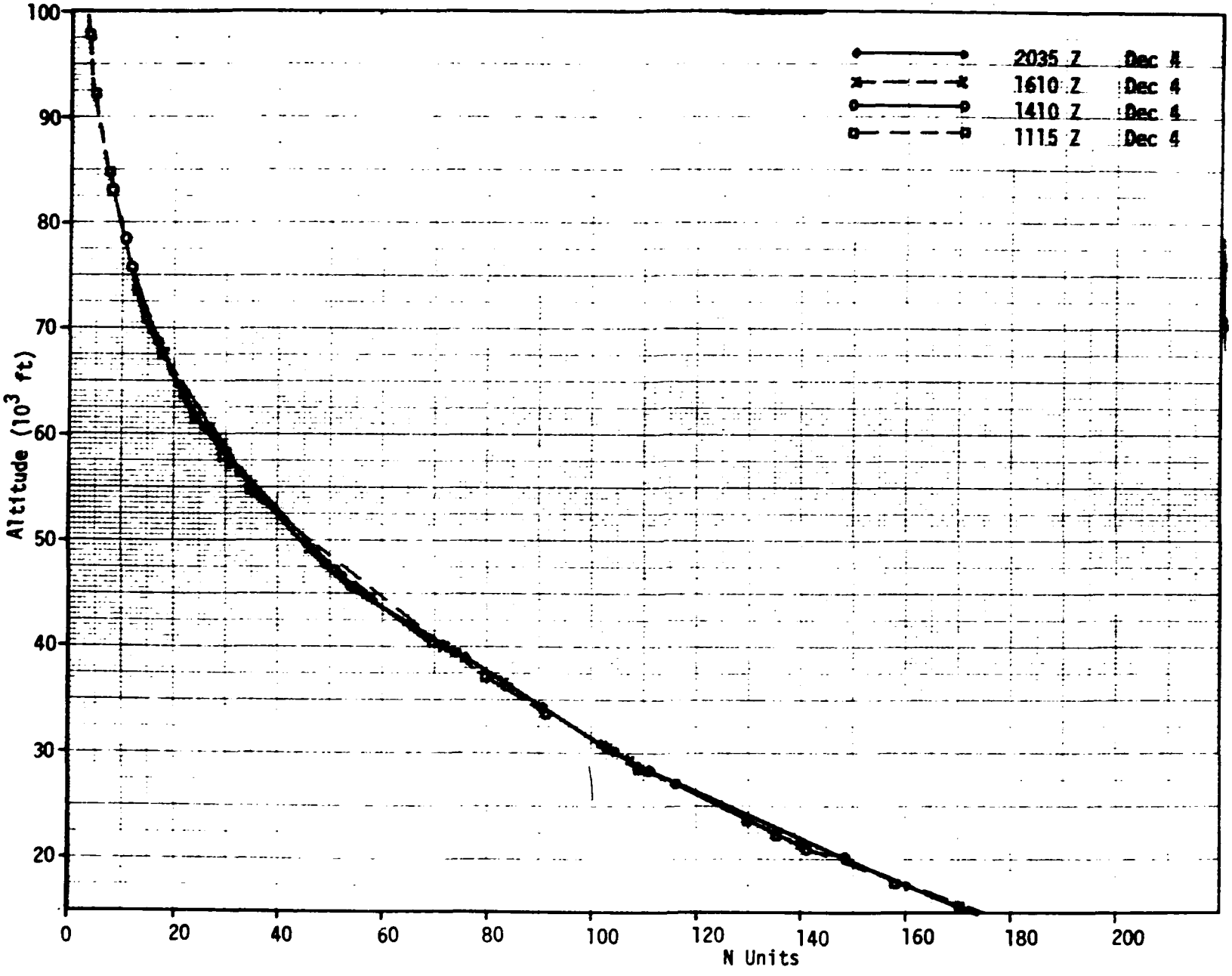

Figure 5.3 (Continued)

5.3 Summary

In view of the discussions in the last two sections, suggestion is made to take either the tropopause or the 30,000 ft, whichever is higher, as the minimum required height for rawinsonde measurements. That is, if the rawinsonde can reach above the minimum height, no additional launch is necessary even though the rawinsonde might not provide measurements up to 100,000 ft. Any gap of missing data which exists between the minimum height and 100,000 ft, should be filled in by using the corresponding part of the data obtained in the previous or the following range-support or synoptic launch. If the data is not available in this way, the seasonal or monthly mean profile should be used. If for any reason the rawinsonde fails to supply good measurements from ground to above the minimum height, a real-time follow-on rawinsonde launch is suggested.

The height of the tropopause varies with the season. The nominal height of the tropopause over the Southern California coastline is around 38,000 ft. Sometimes it might move up to 50,000 ft or might be as low as 25,000 ft.

6.0 CONCLUSIONS AND SUGGESTIONS

6.1 Conclusions

The conclusions of this refraction study must be qualified by the limited sample size (2 operations). But within the qualification of the data presented, the following conclusions can be summarized as follows:

(1) Some postflight refraction corrections were calculated from the annual mean profile given in the SAMTEC West Default Meteorological File and the CRPL exponential profiles extrapolated from the ground measurements. These corrections were compared with the corrections based on the refractivity profiles derived from rawinsonde measurements. It was indicated by the comparison that the local annual mean refractivity profile is a better model to be used for refraction corrections when rawinsonde data is not available. However, the seasonal or monthly mean profile might provide even better results.

(2) It was estimated that the total error of range corrections is less than 4 to 6 percent of the total range correction and the total error of elevation angle correction is less than 3 percent of the total elevation angle correction for measurements made at elevation angles larger than 3.5 degrees. As discussed in Appendix D, the magnitudes of these errors do not exceed the permissible refraction correction errors for SAMTEC West and Mainland radars, except at the beginning or near the end of the tracking.

(3) The tropopause (existing between 25,000 ft and 50,000 ft) or the altitude of 30,000 feet, whichever is higher, should be taken as the minimum height required for rawinsonde measurements in supporting missile launch. Any gap of missing data which exists between the minimum height and 100,000 feet, should be filled in with the corresponding part of the data obtained in the previous or the following range-support or synoptic rawinsonde launch. If the data is not available in this way, the seasonal or monthly mean profile should be used to fill the gap.

It is restated that the above conclusions are based on the results of calculations made for two operations. They are not drawn on a statistical basis.

6.2 Suggestions for Future Study

The following suggestions are made for future study and further development for postflight refraction correction technique:

(1) The permissible refraction correction errors on range and elevation angle adopted in this study were determined from review of noise, granularity, and unmodelled trends shown in the fully corrected metric data for MM III flights. In order to establish the minimum acceptable operational criteria on refraction corrections, the permissible refraction errors should be determined in a more absolute sense by considering the required trajectory accuracy in multisensor solution. A future analysis should be conducted to evaluate the magnitudes of the refraction correction errors which could be propagated into the best estimated trajectory. By comparing the propagated errors with the allowable trajectory state vector errors, the permissible refraction correction errors for range and elevation angle can be determined.

(2) The seasonal and monthly mean refractivity profiles for Vandenberg, Pillar Point and Barking Sands should be obtained and documented. A study should be made to determine the amount of improvement which can be achieved by using the seasonal or monthly mean profile as model profile other than using the grand annual profile given in the SAMTEC Default Meteorological File.

(3) It is recommended that the rawinsonde data reduction program which are currently developed on the computer NOVA 1220 at VAFB should be modified to include the capability to check any gap of missing data in each refractivity profile and to fill the gap with proper data points as described in (3) of Section 6.1.

REFERENCES

1. IRIG Standards for Range Meteorological Data Reduction Part I - Rawinsonde. Document 108-72, Range Commanders Council, White Sands Missile Range, New Mexico, 1972.

2. Effects of Atmospheric Refraction on Microwave Tracking Instrumentation. Document 112-65, Range Commanders Council, White Sands Missile Range, New Mexico, 1965.

3. REFRAC: Refraction Module for the Postflight Data Reduction Software System (Computer Program Detailed Technical Description). SAMTEC REFR-1195-3120-00, Data Processing Directorate, FEC/WTR, 1972.

4. Reliability of Meteorological Data. Document 110-71, Range Commanders Council, White Sands Missile Range, New Mexico, 1971.

5. Airborne Refractometer Data Gathering. SAMTEC TR 72-7, Colin Gardner, Vandenberg AFB, 1972.

6. Comparison of Refraction Correction Techniques. Technical Staff Technical Memo No. 65. ETV-TM-67-2. Charles A. Bjork and William M. Layson, 1967.

7. Comparisons of Radar Refraction Correction Computer Programs at Selected Test Ranges. Document 113-70, Range Commanders Council, White Sands Missile Range, New Mexico, 1970.

8. Private communication with G. D. Trimble about computer program REEK, FEC/WTR, Vandenberg AFB.

9. Private communication with Colin Gardner, ROS/SAMTEC.

10. Rawinsonde Data collected in June and December 1975 by Weather Squadron, Vandenberg AFB.

11. REFRAC: Refraction Correction for Radar. SAMTEC TD-70-0468 System Software and Analysis Organization, FEC/WTR, July 1970.

12. Proceeding of the Second Tropospheric Refraction Effects Technical Review Meeting, Volume II. April 1964. Pages 3-259 to 3-307.

13. CRPL Exponential Reference Atmosphere, NBS Monograph 4, October 29, 1959, with Errata Sheet December 11, 1959.

14. Meteorological Data Error Estimates. Document 110-77, Range Commanders Council, White Sands Missile Range, New Mexico, 1977.

APPENDIX A

TABULATED REFRACTION CORRECTIONS BASED ON RAWINSONDE PROFILES AND SELECTED REFRACTIVITY MODELS

Table A.1 The Differences Between the Refraction Corrections Based On Rawinsonde Profile and Model Profiles (Radar 023003, Vandenberg, Op 6290, July 15, 1976)

T+Time (sec)	E (deg)	R (10^6 ft)	DR_0 (ft)	DR_1 (ft)	DR_{12} (ft)	DE_0 (mils)	DE_1 (mils)	DE_{12} (mils)
20	7.6	0.07	18.01	-1.74	-0.23	0.69806	0.1883	0.0245
30	17.3	0.08	15.11	-0.75	-0.26	0.46533	0.03473	0.01124
40	28.4	0.09	13.32	0.31	-0.16	0.35621	-0.00561	0.00338
50	37.0	0.11	12.31	0.80	-0.01	0.31532	-0.00887	0.00014
60	40.8	0.16	11.84	0.89	0.04	0.31431	-0.00606	-0.00027
70	41.4	0.21	11.83	0.96	0.11	0.33016	-0.00469	-0.00060
80	40.8	0.27	11.99	0.98	0.12	0.35199	-0.00368	-0.00049
90	39.6	0.34	12.26	1.00	0.12	0.37615	-0.00301	-0.00044
100	38.4	0.42	12.60	1.03	0.13	0.40108	-0.00252	-0.00038
120	36.0	0.60	13.29	1.08	0.13	0.44827	-0.00181	-0.00030
140	34.1	0.83	13.96	1.14	0.14	0.49007	-0.00132	-0.00026
160	32.5	1.10	14.53	1.18	0.14	0.52501	-0.00096	-0.00022
180	31.4	1.46	14.97	1.22	0.14	0.55208	-0.00062	-0.00018
200	30.6	1.87	15.33	1.25	0.15	0.57351	-0.00036	-0.00015
300	26.9	3.89	17.22	1.40	0.16	0.67533	0.00012	-0.00012
400	23.4	5.81	19.59	1.58	0.19	0.79318	0.00025	-0.00012
500	19.9	7.59	22.84	1.84	0.22	0.94849	0.00022	-0.00014
600	16.4	9.26	27.42	2.19	0.26	1.16199	-0.00004	-0.00020
700	12.9	10.8	34.36	2.69	0.31	1.47865	-0.00082	-0.00031
800	9.3	12.3	46.27	3.51	0.38	2.01251	-0.00317	-0.00049
840	7.9	12.9	53.46	3.97	0.41	2.33197	-0.00513	-0.00055
880	6.5	13.4	63.62	4.55	0.44	2.78141	-0.00831	-0.00047
920	5.1	13.9	78.23	5.26	0.44	3.42577	-0.01285	0.00022
960	3.6	14.5	100.51	6.03	0.40	4.41053	-0.01509	0.00344
1000	2.1	15.0	141.52	6.51	0.20	6.25950	0.02983	0.02035
1050	0.3	15.6	237.68	7.45	-0.15	11.00539	0.82030	0.09118

DR_0, DE_0 = range and elevation angle corrections based on the measured refractivity profile.

DR_1, DE_1 = differences in range and elevation angle corrections (DR_0, DE_0 minus the corrections based on the CRPL exponential model).

DR_{12}, DE_{12} = differences in range and elevation angle corrections (DR_0, DE_0 minus the corrections based on the mean profile).

Table A.2 The Differences Between the Refraction Corrections Based On Rawinsonde Profile and Model Profiles (Radar 213002, Pillar Point, Op 6290, July 15, 1976)

T+Time (sec)	E (deg)	R (10^6 ft)	DR_0 (ft)	DR_1 (ft)	DR_{12} (ft)	DE_0 (mils)	DE_1 (mils)	DE_{12} (mils)
57	3.5	1.09	106.42	6.07	-0.64	3.65097	-0.03958	0.03448
60	3.9	1.08	95.51	6.03	-0.35	3.32426	-0.04918	0.02136
64	4.7	1.08	83.37	5.72	-0.14	2.96223	-0.04961	0.01168
68	5.5	1.08	73.81	5.45	0.10	2.66975	-0.04601	0.00576
72	6.3	1.07	65.88	5.10	0.22	2.42199	-0.04059	0.00264
76	7.2	1.07	59.18	4.70	0.24	2.20771	-0.03490	0.00112
80	8.0	1.07	53.48	4.33	0.25	2.02009	-0.02976	0.00027
90	10.3	1.07	42.62		0.24			-0.00053
100	12.7	1.07	35.00	2.98	0.21	1.36883	-0.01373	-0.00063
120	17.9	1.09	25.36	2.26	0.17	0.99541	-0.00699	-0.00045
140	22.8	1.16	20.23	1.77	0.15	0.78268	-0.00408	-0.00029
160	26.9	1.29	17.38	1.53	0.13	0.65843	-0.00264	-0.00020
180	29.9	1.52	15.78	1.39	0.12	0.58643	-0.00182	-0.00014
200	31.5	1.84	15.08	1.32	0.11	0.55526	-0.00139	-0.00011
300	29.6	3.66	15.96	1.40	0.12	0.60562	-0.00092	-0.00007
400	25.7	5.50	18.09	1.59	0.13	0.71337	-0.00096	-0.00007
500	21.9	7.25	21.02	1.84	0.15	0.85488	-0.00121	-0.00009
600	18.2	8.89	25.03	2.16	0.17	1.04290	-0.00171	-0.00011
700	14.5	10.4	30.97	2.64	0.20	1.31425	-0.00276	-0.00014
800	10.9	11.9	40.62	3.38	0.24	1.74636	-0.00522	-0.00016
840	9.4	12.4	46.40	3.80	0.24	2.00290	-0.00712	-0.00011
880	7.9	13.0	54.09	4.33	0.25	2.34198	-0.01006	0.00011
920	6.5	13.5	64.79	4.99	0.22	2.81233	-0.01468	0.00085
960	5.0	14.0	80.21	5.78	0.14	3.48888	-0.02113	0.00336
1000	3.5	14.5	105.25	6.63	-0.10	4.59411	-0.02398	0.01375

Table A.3 The Differences Between the Refraction Corrections Based On Rawinsonde Profile and Model Profiles (Radar 023003, Vandenberg, Op 3445, January 21, 1977)

T+Time (sec)	E (deg)	R (10^6 ft)	DR_0 (ft)	DR_1 (ft)	DR_{12} (ft)	DE_0 (mils)	DE_1 (mils)	DE_{12} (mils)
12	2.5	0.07	20.71	0.41	0.43	0.34201	-0.12964	-0.14826
20	7.5	0.07	18.40	0.38	0.91	0.39518	-0.03896	-0.10332
30	16.9	0.07	15.85	0.87	0.84	0.33848	-0.0384	-0.0391
40	27.1	0.08	14.15	1.24	0.54	0.30432	-0.0283	-0.01277
50	34.1	0.11	13.34	1.36	0.37	0.29994	-0.0178	-0.00501
60	36.7	0.15	13.16	1.35	0.34	0.32136	-0.01127	-0.00303
100	32.5	0.42	14.81	1.55	0.43	0.45456	-0.00524	-0.00171
150	25.8	0.97	18.29	1.92	0.54	0.63450	-0.00336	-0.00127
200	21.5	1.92	21.63	2.27	0.64	0.79422	-0.00229	-0.00104
300	16.5	4.02	27.87	2.91	0.82	1.06907	-0.00212	-0.00115
350	14.3	5.05	31.78	3.31	0.93	1.23359	-0.0027	-0.00141
400	12.2	6.05	36.98	3.84	1.08	1.44789	-0.00401	-0.00193
450	10.1	7.02	44.06	4.56	1.29	1.73463	-0.00662	-0.00291
500	8.0	7.98	54.37	5.57	1.60	2.14521	-0.01223	-0.00503
520	7.2	8.35	59.83	6.10	1.77	2.35999	-0.01613	-0.00654
540	6.4	8.73	66.43	6.73	1.97	2.61747	-0.02174	-0.0088
560	5.6	9.10	74.53	7.47	2.22	2.93057	-0.03003	-0.01232
600	4.0	9.83	98.14	9.51	2.97	3.82511	-0.06346	-0.02873
620	3.2	10.2	114.35	10.77	3.49	4.42583	-0.09458	-0.04716
640	2.4	10.5	136.33	12.26	4.20	5.22317	-0.1473	-0.0851
660	1.6	10.9	170.12	14.03	5.17	6.41307	-0.25134	-0.18338
680	0.9	11.3	211.79	15.21	5.79	7.82337	-0.41943	-0.39571

Table A.4 The Differences Between the Refraction Corrections Based On Rawinsonde Profile and Model Profiles (Radar 213002, Pillar Point, Op 3445, January 21, 1977)

T+Time (sec)	E (deg)	R (10^6 ft)	DR_0 (ft)	DR_1 (ft)	DR_{12} (ft)	DE_0 (mils)	DE_1 (mils)	DE_{12} (mils)
60	3.4	1.08	109.22	10.78	3.16	3.34775	-0.09484	-0.07897
64	4.1	1.07	95.25	9.34	2.39	3.02912	-0.06546	-0.05197
68	4.8	1.07	84.25	8.21	1.90	2.76227	-0.04491	-0.03596
72	5.5	1.07	75.20	7.40	1.64	2.52883	-0.03079	-0.02629
76	6.3	1.07	67.76	6.71	1.44	2.32662	-0.02059	-0.01983
80	7.0	1.06	61.31	6.10	1.28	2.14316	-0.01286	-0.01519
90	9.0	1.06	49.13	4.93	0.99	1.77386	-0.00136	-0.00854
100	11.0	1.05	40.60	4.08	0.79	1.49614	0.00409	-0.00528
120	15.2	1.07	29.96	3.03	0.57	1.12375	0.00784	-0.00248
140	18.8	1.13	24.48	2.47	0.46	0.91959	0.00852	-0.00146
160	21.5	1.26	21.66	2.19	0.40	0.81162	0.00871	-0.00099
180	22.8	1.50	20.43	2.07	0.38	0.76634	0.00903	-0.00074
200	23.0	1.82	20.31	2.06	0.38	0.76710	0.00958	-0.00062
300	18.6	3.73	24.73	2.50	0.46	0.97446	0.01307	-0.00060
400	14.0	5.69	32.44	3.27	0.62	1.31124	0.01708	-0.00099
450	11.7	6.65	38.24	3.85	0.74	1.55809	0.01936	-0.00148
500	9.5	7.59	46.46	4.66	0.92	1.90181	0.02161	-0.00251
540	7.8	8.33	55.66	5.56	1.14	2.28075	0.02271	-0.00428
580	6.1	9.06	68.86	6.82	1.48	2.81607	0.02148	-0.00832
600	5.3	9.41	77.89	7.65	1.72	3.17715	0.01867	-0.01238
620	4.4	9.77	89.42	8.68	2.04	3.63321	0.01278	-0.01954
640	3.6	10.1	104.74	9.97	2.51	4.23051	0.00117	-0.03328
660	2.8	10.5	124.69	11.50	3.13	4.99625	-0.01948	-0.0604
680	2.0	10.8	151.15	13.25	3.93	5.99547	-0.0532	-0.11736

APPENDIX B

TABULATED METEOROLOGICAL PARAMETERS AND REFRACTIVITY ERRORS

Table B.1 Meteorological Parameters, Refractivity, and the Errors at Significant Levels from Rawinsonde Measurements at Vandenberg for Op 6290 (July 15, 1976)

	H (ft)	T (°C)	RH (%)	P (mb)	N	A	B	C	ΔT (°C)	Δ(RH) (%)	ΔP (mb)	ΔN
1	000327	13.9	100.00	1002.5	343	-1.45	4.51	0.27	0.3	3.0	0.3	4.06
2	001469	12.1	100.00	962.0	326	-1.37	4.57	0.27	1.0	5.0	1.9	9.36
3	001876	15.0	82.79	948.0	319	-1.33	4.48	0.27	1.0	5.0	1.9	9.72
4	002053	14.4	78.43	942.0	312	-1.29	4.49	0.27	1.0	5.0	1.9	9.23
5	002680	16.0	30.77	921.0	272	-1.03	4.44	0.27	1.0	5.0	1.8	7.14
6	003769	20.2	6.41	886.0	241	-0.84	4.32	0.26	1.0	5.0	1.8	6.84
7	004253	22.8	0.0	871.0	228	-0.77	4.24	0.26	1.0	5.0	1.7	7.11
8	004714	22.2	0.0	857.0	225	-0.76	4.26	0.26	1.0	5.0	1.7	6.91
9	005722	19.1	24.93	827.0	244	-0.92	4.35	0.27	1.0	5.0	1.7	7.67
10	006724	16.4	28.07	798.0	237	-0.90	4.43	0.27	1.0	5.0	1.6	6.94
11	007647	15.0	17.99	772.0	222	-0.82	4.48	0.27	1.0	5.0	1.5	5.92
12	008672	14.3	0.0	744.0	201	-0.70	4.50	0.27	1.0	5.0	1.5	4.77
13	010582	9.9	0.0	694.0	190	-0.67	4.64	0.27	1.0	5.0	1.4	3.89
14	011537	7.2	6.92	670.0	189	-0.69	4.73	0.28	1.0	5.0	1.3	3.68
15	012601	4.8	6.00	644.0	182	-0.66	4.81	0.28	1.0	5.0	1.3	3.27
16	013527	1.6	7.97	622.0	178	-0.66	4.92	0.28	1.0	5.0	1.2	2.88
17	014656	0.8	5.15	596.0	170	-0.63	4.95	0.28	1.0	5.0	1.2	2.69
18	015644	-1.6	0.0	754.0	164	-0.60	5.04	0.29	1.0	10.0	1.1	3.66

Table B.1 (Continued)

	H (ft)	T (°C)	RH (%)	P (mb)	N	A	B	C	ΔT (°C)	Δ(RH) (%)	ΔP (mb)	ΔN
19	016662	-5.0	9.09	552.0	161	-0.61	5.17	0.29	1.0	10.0	1.1	3.26
20	017711	-7.2	30.99	530.0	160	-0.63	5.26	0.29	1.0	10.0	1.1	3.27
21	018796	-8.2	0.0	508.0	149	-0.56	5.30	0.29	1.0	10.0	1.0	2.60
22	019815	-11.4	5.70	488.0	145	-0.56	5.43	0.30	1.0	10.0	1.0	2.31
23	026262	-27.1	7.28	375.0	119	-0.48	6.15	0.32	1.0	15.0	1.0	1.43
24	028427	-31.2	6.43	342.0	110	-0.45	6.36	0.32	1.0	20.0	1.0	1.36
25	029541	-33.1	0.0	326.0	105	-0.44	6.46	0.32	1.0	20.0	1.0	1.24
26	030480	-34.8	0.0	313.0	102	-0.43	6.55	0.33	1.0	20.0	0.9	1.13
27	034768	-42.6	0.0	259.0	87	-0.38	7.00	0.34	1.0	20.0	0.8	0.84
28	047403	-63.8	0.0	143.0	53	-0.25	8.50	0.37	1.0	20.0	0.8	0.57
29	051102	-66.6	0.0	119.0	45	-0.22	8.73	0.38	1.0	20.0	0.7	0.49
30	056024	-67.8	0.0	93.0	35	-0.17	8.83	0.38	1.0	20.0	0.6	0.41
31	075587	-51.4	0.0	36.0	13	-0.06	7.57	0.35	1.5	20.0	0.4	0.30
32	078792	-52.3	0.0	31.0	11	-0.05	7.63	0.35	2.5	20.0	0.3	0.30
33	086209	-48.2	0.0	22.0	8	-0.03	7.36	0.34	2.5	20.0	0.2	0.26
34	100615	-40.2	0.0	11.5	4	-0.02	6.86	0.33	2.5	20.0	0.1	0.32
35	109429	-38.9	0.0	7.8	3	-0.01	6.78	0.33	2.5	20.0	0.1	0.34

Table B.2 Meteorological Parameters, Refractivity, and the Errors at Significant Levels from Rawinsonde Measurements at Point Pillar for Op 6290 (July 15, 1976)

	H (ft)	T (°C)	RH (%)	P (mb)	N	A	B	C	ΔT (°C)	Δ(RH) (%)	ΔP (mb)	ΔN
1	000161	13.1	100.00	1009.0	342	-1.44	4.54	0.27	0.3	3.0	0.3	3.90
2	001916	9.7	100.00	947.0	316	-1.32	4.65	0.27	1.0	5.0	1.8	8.36
3	001975	12.7	15.29	945.0	268	-0.97	4.55	0.27	1.0	5.0	1.8	5.47
4	002273	20.9	0.0	935.0	247	-0.84	4.30	0.26	1.0	5.0	1.8	6.63
5	003237	23.4	0.0	904.0	237	-0.80	4.22	0.26	1.0	5.0	1.8	7.35
6	004238	22.7	11.03	873.0	242	-0.86	4.24	0.26	1.0	5.0	1.7	7.95
7	005238	21.3	8.44	843.0	231	-0.82	4.29	0.26	1.0	5.0	1.7	7.26
8	006201	21.1	0.0	815.0	215	-0.73	4.29	0.26	1.0	5.0	1.6	6.52
9	007194	19.2	5.75	787.0	214	-0.75	4.35	0.27	1.0	5.0	1.5	6.34
10	009198	15.7	5.09	733.0	201	-0.71	4.45	0.27	1.0	5.0	1.4	5.32
11	012013	9.0	7.49	662.0	186	-0.67	4.67	0.28	1.0	5.0	1.3	3.98
12	015527	-0.3	45.95	581.0	179	-0.71	4.99	0.28	1.0	5.0	1.1	3.51
13	015801	-0.8	33.89	575.0	174	-0.67	5.01	0.28	1.0	10.0	1.1	4.59
14	016686	-2.4	0.0	556.0	159	-0.59	5.07	0.29	1.0	10.0	1.1	3.50
15	023401	-18.6	0.0	427.0	130	-0.51	5.74	0.30	1.0	10.0	1.1	1.65
16	025186	-21.7	0.0	397.0	123	-0.49	5.88	0.31	1.0	15.0	1.0	1.74
17	026058	-24.3	9.74	383.0	120	-0.48	6.01	0.31	1.0	20.0	1.0	1.86
18	028750	-31.5	7.22	342.0	110	-0.46	6.37	0.32	1.0	20.0	1.0	1.35

Table B.2 (Continued)

		T	RH	P	N	A	B	C	ΔT	Δ(RH)	ΔP	ΔN
		(°C)	(%)	(mb)					(°C)	(%)	(mb)	
	295285	-32.8	0.0	330.0	107	-0.44	6.44	0.32	1.0	20.0	1.0	1.26
	310519	-34.8	0.0	317.0	103	-0.43	6.55	0.33	1.0	20.0	1.9	1.14
	331331	-37.5	0.0	306.0	101	-0.43	6.70	0.33	1.0	20.0	0.9	1.04
	335334	-47.0	0.0	256.0	87	-0.39	7.28	0.34	1.0	20.0	0.8	0.79
	039354	-49.6	0.0	213.0	74	-0.33	7.45	0.35	1.0	20.0	0.6	0.63
24	049997	-66.3	0.0	128.0	48	-0.23	8.71	0.38	1.0	20.0	0.6	0.47
25	051464	-67.1	0.0	119.0	45	-0.22	8.77	0.38	1.0	20.0	0.6	0.46
26	057083	-66.3	0.0	90.0	34	-0.16	8.71	0.38	1.0	20.0	0.5	0.36
27	062777	-63.9	0.0	68.0	25	-0.12	8.51	0.37	1.0	20.0	0.4	0.29
28	064357	-58.8	0.0	63.0	23	-0.11	8.11	0.36	1.0	20.0	0.4	0.28
29	068369	-58.8	0.0	52.0	19	-0.09	8.11	0.36	1.0	20.0	0.3	0.23
30	071899	-54.1	0.0	44.0	16	-0.07	7.76	0.35	1.5	20.0	0.3	0.27
31	102476	-39.5	0.0	11.0	4	-0.02	6.82	0.33	2.5	20.0	0.1	0.34
32	105114	-39.3	0.0	9.8	3	-0.01	6.81	0.33	2.5	20.0	0.1	0.34

Table B.3 Refractivity Errors Caused by Uncertainties in Temperature, Water Vapor, and Pressure Measurements at Vandenberg for Op 6290

	H (ft)	A·ΔT	B·ΔE	C·ΔP
1	00327	0.43	3.55	0.08
2	001469	1.37	7.48	0.52
3	001876	1.33	7.89	0.51
4	002053	1.29	7.43	0.51
5	002680	1.03	5.63	0.48
6	003769	0.84	5.52	0.48
7	004253	0.77	5.89	0.45
8	004714	0.76	5.70	0.45
9	005722	0.92	6.31	0.45
10	006724	0.90	5.61	0.43
11	007647	0.82	4.70	0.40
12	008672	0.70	3.67	0.40
13	010582	0.67	2.83	0.38
14	011537	0.69	2.63	0.36
15	012601	0.66	2.24	0.36
16	013527	0.66	1.88	0.34
17	014656	0.63	1.72	0.34
18	015644	0.60	2.74	0.31
19	016662	0.61	2.33	0.32
20	017711	0.63	2.32	0.32
21	018796	0.56	1.74	0.29
22	019815	0.56	1.45	0.30
23	026262	0.48	0.64	0.32
24	028427	0.45	0.59	0.32
25	029541	0.44	0.48	0.32
26	030480	0.43	0.41	0.29
27	034768	0.38	0.20	0.27
28	047403	0.25	0.02	0.30
29	051102	0.22	0.01	0.26
30	056024	0.17	0.01	0.23
31	075587	0.09	0.08	0.14
32	078792	0.12	0.07	0.11
33	086209	0.08	0.11	0.07
34	100615	0.04	0.25	0.03
35	109429	0.03	0.28	0.03

Table B.4 Refractivity Errors Caused by Uncertainties in Temperature, Water Vapor, and Pressure Measurements at Point Pillar for Op 6290

	H (ft)	A•ΔT	B•ΔE	C•ΔP
1	000161	0.43	3.39	0.08
2	001916	1.32	6.55	0.49
3	001975	0.97	4.01	0.49
4	002273	0.84	5.31	0.48
5	003237	0.80	6.08	0.47
6	004238	0.86	6.64	0.45
7	005238	0.82	5.99	0.45
8	006201	0.73	5.37	0.42
9	007194	0.75	5.18	0.40
10	009198	0.71	4.23	0.38
11	012013	0.67	2.95	0.36
12	015527	0.71	2.49	0.31
13	015801	0.67	3.61	0.31
14	016686	0.59	2.60	0.32
15	023401	0.51	0.81	0.34
16	025186	0.49	0.95	0.31
17	026058	0.48	1.07	0.31
18	028750	0.46	0.57	0.32
19	029585	0.44	0.49	0.32
20	030519	0.43	0.41	0.29
21	031331	0.43	0.32	0.30
22	035334	0.39	0.12	0.27
23	039354	0.33	0.09	0.21
24	049997	0.23	0.01	0.23
25	051464	0.22	0.01	0.23
26	057083	0.16	0.01	0.19
27	062777	0.12	0.02	0.15
28	064357	0.11	0.03	0.14
29	068369	0.09	0.03	0.11
30	071899	0.11	0.06	0.11
31	102476	0.04	0.26	0.03
32	105114	0.03	0.27	0.03

APPENDIX C

TABULATED ERRORS IN REFRACTION CORRECTIONS

Table C.1 Errors in Refraction Corrections Based on Rawinsonde Measurements (Radar 213002, Pillar Point, Op 6290, July 15, 1976)

T+Time (sec)	E (deg)	R (10^6 ft)	DR_0 (ft)	DR_2 (ft)	DR_3 (ft)	DR_4 (ft)	DR_5 (ft)
57	3.5	1.09	106.42	-2.05	2.2	0.18	0.09
60	3.9	1.08	95.51	-1.82	2.05	0.19	0.14
64	4.7	1.08	83.37	-1.65	1.8	0.19	0.05
68	5.5	1.08	73.81	-1.51	1.58	0.17	-0.02
72	6.3	1.07	65.88	-1.37	1.41	0.16	-0.05
76	7.2	1.07	59.18	-1.23	1.27	0.15	-0.05
80	8.0	1.07	53.48	-1.11	1.15	0.14	-0.05
90	10.3	1.07	42.62	-0.88	0.92	0.12	-0.04
100	12.7	1.07	35.00	-0.73	0.75	0.08	-0.04
120	17.9	1.09	25.36	-0.53	0.55	0.07	-0.03
140	22.8	1.16	20.23	-0.42	0.44	0.06	-0.02
160	26.9	1.29	17.38	-0.36	0.38	0.05	-0.02
180	29.9	1.52	15.78	-0.33	0.34	0.05	-0.02
200	31.5	1.84	15.08	-0.32	0.32	0.04	-0.02
300	29.6	3.66	15.95	-0.33	0.34	0.05	-0.02
400	25.7	5.50	18.09	-0.38	0.39	0.05	-0.02
500	21.9	7.25	21.02	-0.44	0.45	0.06	-0.02
600	18.2	8.89	25.03	-0.53	0.54	0.07	-0.03
700	14.5	10.4	30.97	-0.65	0.66	0.08	-0.04
800	10.9	11.9	40.62	-0.84	0.88	0.12	-0.04
840	9.4	12.4	46.40	-0.97	1.00	0.12	-0.04
880	7.9	13.0	54.09	-1.12	1.17	0.14	-0.04
920	6.5	13.5	64.79	-1.35	1.39	0.16	-0.05
960	5.0	14.0	80.21	-1.68	1.72	0.18	-0.05
1000	3.5	14.5	105.25	-2.21	2.27	0.20	-0.02

DR_0 = range correction based on the measured refractivity profile.

DR_2, DR_3 = error in range correction (DR_0 minus the corrections based on the outer bounding and inner bounding erroneous refractivity profile).

DR_4, DR_5 = error in range correction (DR_0 minus the corrections based on the two zigzag erroneous curves).

Table C.1 (Continued)

T+Time (sec)	E (deg)	R (10^6 ft)	DE_0 (Mils)	DE_2 (Mils)	DE_3 (Mils)	DE_4 (Mils)	DE_5 (Mils)
57	3.5	1.09	3.65097	-0.02404	0.02291	-0.07315	0.06889
60	3.9	1.08	3.32426	-0.02525	0.02345	-0.06227	0.05821
64	4.7	1.08	2.96223	-0.02462	0.02352	-0.05162	0.04900
68	5.5	1.08	2.66975	-0.02346	0.02284	-0.04408	0.04237
72	6.3	1.07	2.42199	-0.02222	0.02183	-0.03828	0.03707
76	7.2	1.07	2.20771	-0.02101	0.02067	-0.03368	0.03272
80	8.0	1.07	2.02009	-0.01976	0.01948	-0.02991	0.02915
90	10.3	1.07		-0.01686	0.01668	-0.02307	0.02260
100	12.7	1.07	1.36883	-0.01443	0.01431	-0.01848	0.01818
120	17.9	1.09	0.99541	-0.01086	0.01080	-0.01282	0.01267
140	22.8	1.16	0.78268	-0.00869	0.00866	-0.00982	0.00973
160	26.9	1.29	0.65843	-0.0074	0.00737	-0.00812	0.00806
180	29.9	1.52	0.58643	-0.00664	0.00663	-0.00713	0.00711
200	31.5	1.84	0.55526	-0.00633	0.00631	-0.00670	0.00667
300	29.6	3.66	0.60562	-0.00696	0.00696	-0.00721	0.00720
400	25.7	5.50	0.71337	-0.00821	0.00821	-0.00847	0.00846
500	21.9	7.25	0.85488	-0.00985	0.00983	-0.01018	0.01014
600	18.2	8.89	1.04290	-0.01199	0.01197	-0.01246	0.01242
700	14.5	10.4	1.31425	-0.01504	0.01502	-0.01583	0.01578
800	10.9	11.9	1.74636	-0.01982	0.01977	-0.02140	0.02128
840	9.4	12.4	2.00290	-0.02259	0.02252	-0.02486	0.02468
880	7.9	13.0	2.34198	-0.02617	0.02606	-0.02960	0.02933
920	6.5	13.5	2.81233	-0.03091	0.03076	-0.03660	0.03615
960	5.0	14.0	3.48888	-0.03716	0.03695	-0.04766	0.04687
1000	3.5	14.5	4.59411	-0.04528	0.04497	-0.06910	0.06732

DE_0 = elevation angle correction based on the measured refractivity profile

DE_2, DE_3 = error in elevation angle correction (DE_0 minus the corrections based on the outer and inner bounding erroneous refractivity profiles).

DE_4, DE_5 = error in elevation angle correction (DE_0 minus the corrections based on the two zigzag erroneous curves).

Table C.2 Errors in Refraction Corrections Based on Rawinsonde Measurements (Radar 023003, Vandenberg, Op 6290, July 15, 1976)

T+Time (sec)	E (deg)	R (10^6 ft)	DR_0 (ft)	DR_2 (ft)	DR_4 (ft)	DE_0 (mils)	DE_2 (mils)	DE_4 (mils)
20	7.6	0.07	18.01	- 0.48	0.04	0.69806	0.02043	-0.0349
30	17.3	0.08	15.11	- 0.36	0.03	0.46533	0.00236	-0.01424
40	28.4	0.09	13.32	- 0.27	0.00	0.35621	-0.00169	-0.00766
50	37.0	0.11	12.31	- 0.24	0.01	0.31532	-0.00247	-0.00556
60	40.8	0.16	11.84	- 0.22	0.01	0.31431	-0.003	-0.00481
70	41.4	0.21	11.83	- 0.22	0.01	0.33016	-0.00337	-0.00469
80	40.8	0.27	11.99	- 0.22	0.01	0.35199	-0.00371	-0.00478
90	39.6	0.34	12.26	- 0.23	0.01	0.37615	-0.00406	-0.00496
100	38.4	0.42	12.60	- 0.23	0.02	0.40108	-0.00438	-0.00518
120	36.0	0.60	13.29	- 0.25	0.01	0.44827	-0.00499	-0.00563
140	34.1	0.83	13.96	- 0.26	0.02	0.49007	-0.00552	-0.00605
160	32.5	1.10	14.53	- 0.28	0.01	0.52501	-0.00595	-0.00641
180	31.4	1.46	14.97	- 0.28	0.01	0.55208	-0.00629	-0.00667
200	30.6	1.87	15.33	- 0.28	0.02	0.57351	-0.00656	-0.00689
300	26.9	3.89	17.22	- 0.33	0.02	0.67533	-0.00778	-0.00803
400	23.4	5.81	19.59	- 0.37	0.02	0.79318	-0.00915	-0.00942
500	19.9	7.59	22.84	- 0.43	0.03	0.94849	-0.01093	-0.01127
600	16.4	9.26	27.42	- 0.51	0.03	1.16199	-0.01337	-0.01388
700	12.9	10.8	34.36	- 0.65	0.04	1.47865	-0.01694	-0.01783
800	9.3	12.3	46.27	- 0.88	0.05	2.01251	-0.0228	-0.0248
840	7.9	12.9	53.46	- 1.02	0.05	2.33197	-0.02621	-0.02921
880	6.5	13.4	63.62	- 1.23	0.05	2.78141	-0.0308	-0.03573
920	5.1	13.9	78.23	- 1.53	0.05	3.42577	-0.03689	-0.04594
960	3.6	14.5	100.51	- 1.99	0.04	4.41053	-0.04454	-0.06393
1000	2.1	15.0	141.52	- 2.88	-0.06	6.25950	-0.04991	-0.10891
1050	0.3	15.6	237.68	- 4.54	-1.40	11.00539	0.05516	-0.36761

Table C.3 Errors in Refraction Corrections Based on Rawinsonde Measurements (Radar 213002, Pillar Point, Op 3445, January 21, 1977)

T+Time (sec)	E (deg)	R (10^6 ft)	DR_0 (ft)	DR_2 (ft)	DR_4 (ft)	DE_0 (mils)	DE_2 (mils)	DE_4 (mils)
60	3.4	1.08	109.22	-1.90	-0.16	3.34775	-0.01138	-0.04893
64	4.1	1.07	95.25	-1.66	-0.14	3.02912	-0.01393	-0.04079
68	4.8	1.07	84.25	-1.46	-0.11	2.76227	-0.01492	-0.03501
72	5.5	1.07	75.20	-1.30	-0.10	2.52883	-0.01512	-0.03056
76	6.3	1.07	67.76	-1.18	-0.09	2.32662	-0.01491	-0.02709
80	7.0	1.06	61.31	-1.07	-0.08	2.14316	-0.01447	-0.02419
90	9.0	1.06	49.13	-0.85	-0.06	1.77386	-0.01301	-0.01894
100	11.0	1.05	40.60	-0.71	-0.05	1.49614	-0.01152	-0.01541
120	15.2	1.07	29.96	-0.52	-0.04	1.12375	-0.00913	-0.01109
140	18.8	1.13	24.48	-0.43	-0.03	0.91959	-0.00767	-0.00886
160	21.5	1.26	21.66	-0.38	-0.03	0.81162	-0.00689	-0.00771
180	22.8	1.50	20.43	-0.35	-0.02	0.76634	-0.00658	-0.00720
200	23.0	1.82	20.31	-0.35	-0.03	0.76710	-0.00664	-0.00716
300	18.6	3.73	24.73	-0.43	-0.03	0.97446	-0.00853	-0.00902
400	14.0	5.69	32.44	-0.56	-0.04	1.31124	-0.01143	-0.0122
450	11.7	6.65	38.24	-0.67	-0.05	1.55809	-0.0135	-0.01461
500	9.5	7.59	46.46	-0.81	-0.06	1.90181	-0.01629	-0.01807
540	7.8	8.33	55.66	-0.97	-0.07	2.28075	-0.01922	-0.02207
580	6.1	9.06	68.86	-1.20	-0.09	2.81607	-0.02304	-0.02812
600	5.3	9.41	77.89	-1.36	-0.10	3.17715	-0.02533	-0.03251
620	4.4	9.77	89.42	-1.57	-0.13	3.63321	-0.02783	-0.03851
640	3.6	10.1	104.74	-1.84	-0.16	4.23051	-0.03024	-0.04728
660	2.8	10.5	124.69	-2.19	-0.20	4.99625	-0.0314	-0.06047
680	2.0	10.8	151.15	-2.67	-0.30	5.99547	-0.02826	-0.08213

Table C.4 Errors in Refraction Corrections Based on Rawinsonde Measurements (Radar 023003, Vandenberg, Op 3445, January 21, 1977)

T+Time (sec)	E (deg)	R (10^6 ft)	DR_0 (ft)	DR_2 (ft)	DR_4 (ft)	DE_0 (mils)	DE_2 (mils)	DE_4 (mils)
12	2.5	0.07	20.71	-0.55	0.08	0.34201	0.1218	0.10025
20	7.5	0.07	18.40	-0.43	0.01	0.39518	0.02495	-0.02447
30	16.9	0.07	15.85	-0.34	0.00	0.33848	0.00588	-0.00993
40	27.1	0.08	14.15	-0.26	0.01	0.30432	0.00028	-0.00607
50	34.1	0.11	13.34	-0.22	0.02	0.29994	-0.00141	-0.00478
60	36.7	0.15	13.16	-0.23	0.00	0.32136	-0.00198	-0.00412
100	32.5	0.42	14.81	-0.31	0.00	0.45456	-0.00356	-0.00478
150	25.8	0.97	18.29	-0.38	0.00	0.63450	-0.00541	-0.00632
200	21.5	1.92	21.63	-0.45	0.00	0.79422	-0.00700	-0.00774
300	16.5	4.02	27.87	-0.59	0.00	1.06907	-0.00955	-0.01035
350	14.3	5.05	31.78	-0.67	-0.01	1.23359	-0.01099	-0.01198
400	12.2	6.05	36.98	-0.78	-0.01	1.44789	-0.01282	-0.01415
450	10.1	7.02	44.06	-0.92	-0.01	1.73463	-0.01518	-0.01716
500	8.0	7.98	54.37	-1.13	-0.01	2.14521	-0.01836	-0.02169
520	7.2	8.35	59.83	-1.24	-0.01	2.35999	-0.01993	-0.02419
540	6.4	8.73	66.43	-1.37	-0.01	2.61747	-0.02169	-0.02731
560	5.6	9.10	74.53	-1.54	-0.02	2.93057	-0.02365	-0.03131
600	4.0	9.83	98.14	-2.01	-0.04	3.82511	-0.02772	-0.04432
620	3.2	10.2	114.35	-2.34	-0.07	4.42583	-0.02865	-0.05473
640	2.4	10.5	136.33	-2.77	-0.12	5.22317	-0.02643	-0.07138
660	1.6	10.9	170.12	-3.40	-0.26	6.41307	-0.01104	-0.10519
680	0.9	11.3	211.79	-4.03	-0.60	7.82337	0.04391	-0.16968

APPENDIX D

PERMISSIBLE REFRACTION CORRECTION ERRORS FOR SAMTEC RADARS

The question arises as to what should be the accuracy goal for radar refraction correction in post flight data reduction. To answer this question one would examine such things as the radar's present accuracy in terms of random and systematic errors. The refraction error should not be allowed to become the dominant error source. Analyses have been made of the C-band radar random and systematic error content in the Post Launch Instrumentation Accuracy Report (PLIAR). The radar beacon tracking accuracies are further summarized in a report entitled Metric Sensor Performance History Report. One useful statistic that is presented in this report is the root-mean-square (RMS) of residuals. That is, the radar data are corrected for all known systematic errors and corrected for any systematic errors as a result of the post flight regression analysis process. The RMS is then formed between this fully corrected radar data and the Best Estimate of Trajectory (BET) transformed to radar coordinates. Thus, if the radar data were trend free as compared to the BET, the RMS would be a measure of the random error content of the data (i.e. in this case it would be equal to one standard deviation of the random error). Trends remaining in the radar data would inflate the RMS to include deviations about the trends as well as random errors. Table D.1 lists the RMS values for range, azimuth and elevation for the SAMTEC radars. These results are for Minuteman III flight. For convenience, an average RMS has been calculated for each system. One can observe that for the range channel the average RMS is approximately 6 feet for all radars. For the elevation measurement, the average RMS values are approximately as follows: 0.08 mil for the MIPIR radars (TPQ-18 and FPQ-6), 0.10 to 0.15 mil for the FPS-16 and FPQ-14 radars, and 0.25 mil for the MPS-36 radars. These values are equal to or larger than the granularities for each radar system.

As a somewhat arbitrary limit, it would be desirable to attempt to maintain the residual refraction error to about 20% of the RMS values. The values of 20 percent of the average RMS values are approximately equal to the residual refraction error limits of .03 mil elevation and 2 feet range that was previously mentioned in the report for tracking conditions above 5 degrees elevation. In the case of the elevation data of the MPS-36 radar, because of the higher noise a larger permissible elevation refraction error of 0.05 mil should be acceptable.

Table D.1

The RMS and Averages of Residual Errors for SAMTEC Radars

Radar Site	Operation Number	Launch Date	Type of Vehicle	Range (feet)	Azimuth (mils)	Elevation (mils)
South VAFB	4172	6 Feb 76	MM III RV-1	3	.10	.11
FPS-16	5280	4 Mar 76	MM III RV-1	4	.11	.11
023001	4044	21 Jun 76	MM III RV-1	5	.21	.09
	7090	30 Jun 76	MM III RV-1	5	.16	.13
	6290	15 Jul 76	MM III RV-1	6	.16	.13
	Average RMS			4.6	0.148	0.114
South VAFB	4172	6 Feb 76	MM III PBV	5	.14	.16
FPS-16	5280	4 Mar 76	MM III PBV	4	.07	.04
023002	4044	21 Jun 76	MM III PBV	10	.19	.17
	7090	30 Jun 75	MM III PBV	5	.12	.12
	6290	15 Jul 76	MM III PBV	5	.12	.10
	Average RMS			5.8	0.128	0.118
South VAFB	4172	6 Feb 76	MM III PBV	6	.10	.08
TPQ-18	5280	4 Mar 76	MM III PBV	5	.07	.10
023003	4044	21 Jun 76	MM III PBV	4	.04	.05
	7090	30 Jun 76	MM III PBV	14	.08	.08
	6290	15 Jul 76	MM III PBV	6	.10	.11
	Average RMS			7	0.078	0.084

Table D.1 (Continued)

Radar Site	Operation Number	Launch Date	Type of Vehicle	Range (feet)	Azimuth (mils)	Elevation (mils)
Pillar Point	4172	6 Feb 76	MM III PV1	4	.09	.10
FPS-16	5280	4 Mar 76	MM III RV1	6	.10	.16
213001	4044	21 Jun 76	MM III RV1	5	.10	.11
	7090	30 Jun 76	MM III RV1	7	.11	.13
	6290	15 Jul 76	MM III RV1	6	.12	.14
	Average RMS			5.6	0.104	0.128
Pillar Point	4172	6 Feb 76	MM III PBV	7	.08	.06
FPQ-6	5280	4 Mar 76	MM III PBV	6	.08	.07
213002	4044	21 Jun 76	MM III PBV	6	.07	.07
	7090	30 Jun 76	MM III PBV	5	.07	.05
	6290	15 Jul 76	MM III PBV	6	.11	.17
	Average RMS			6	0.082	0.084
Pillar Point	4172	6 Feb 76	MM III RV-2	5	.22	.20
MPS-36	5280	4 Mar 76	MM III RV-3	5	.22	.22
213004	4044	21 Jun 76				
	7090	30 Jun 76				
	6290	15 Jul 76	MM III RV-2	6	.29	.33
	Average RMS			5.3	0.243	0.25

Table D.1 (Continued)

Radar Site	Operation Number	Launch Date	Type of Vehicle	Range (feet)	Azimuth (mils)	Elevation (mils)
Kaena Point	4172	6 Feb 76	MM III RV-1	11	.26	.24
FPQ-14	5280	4 Mar 76				
313001	4044	21 Jun 76	MM III RV-1	7	.10	.14
	7090	30 Jun 76	MM III RV-1	7	.13	.09
	6290	15 Jul 76	MM III PBV	4	.10	.06
	Average RMS			7.25	0.148	0.133

No absolute answer exists as to the permissible upper limit of C-band radar refraction correction. The values suggested above appear to be easily obtainable by present day post flight data reduction methods outlined in this report. In addition, these values would appear to be a reasonable apportionment of the remaining RMS residual radar error.

APPENDIX E

TABULATED REFRACTION CORRECTIONS BASED ON THE PROFILES WITH DIFFERENT CUTOFF HEIGHTS

Table E.1 The Differences Between Refraction Corrections Based on the Profiles with Different Cutoff Heights and the Original Profile (Radar 023003, Vandenberg, Op 6290, July 15, 1976)

T+Time (sec)	E (deg)	R (10^6 ft)	DR_0 (ft)	DR_7 (ft)	DR_8 (ft)	DR_9 (ft)	DR_{10} (ft)	DR_{11} (ft)
20	7.6	0.07	18.01	0.00	0.00	0.00	0.00	0.00
30	17.3	0.08	15.11	-0.19	0.00	0.00	0.00	0.06
40	28.4	0.09	13.32	-1.48	-0.23	0.00	0.01	0.06
50	37.0	0.11	12.31	-3.23	-1.31	-0.04	0.12	0.16
60	40.8	0.16	11.84	-3.97	-1.83	-0.15	0.16	0.20
70	41.4	0.21	11.83	-3.81	-1.69	-0.02	0.23	0.27
80	40.8	0.27	11.99	-3.85	-1.71	-0.02	0.24	0.28
90	39.6	0.34	12.26	-3.94	-1.75	-0.02	0.24	0.28
100	38.4	0.42	12.60	-4.04	-1.79	-0.02	0.25	0.30
120	36.0	0.60	13.29	-4.27	-1.90	-0.03	0.26	0.31
140	34.1	0.83	13.96	-4.48	-1.99	-0.02	0.28	0.33
160	32.5	1.10	14.53	-4.66	-2.07	-0.03	0.29	0.34
180	31.4	1.46	14.97	-4.8	-2.13	-0.03	0.30	0.35
200	30.6	1.87	15.33	-4.91	-2.17	-0.02	0.31	0.36
300	26.9	3.89	17.22	-5.51	-2.45	-0.03	0.34	0.40
400	23.4	5.81	19.59	-6.26	-2.78	-0.04	0.38	0.45
500	19.9	7.59	22.84	-7.27	-3.22	-0.04	0.44	0.53
600	16.4	9.26	27.42	-8.68	-3.84	-0.05	0.54	0.63
700	12.9	10.8	34.36	-10.78	-4.77	-0.07	0.66	0.78
800	9.3	12.3	46.27	-14.23	-6.27	-0.10	0.86	1.02
840	7.9	12.9	53.46	-16.21	-7.13	-0.12	0.96	1.15
880	6.5	13.4	63.62	-18.84	-8.26	-0.15	1.10	1.31
920	5.1	13.9	78.23	-22.25	-9.70	-0.20	1.27	1.53
960	3.6	14.5	100.51	-26.59	-11.47	-0.26	1.47	1.81
1000	2.1	15.0	141.52	-32.00	-13.58	-0.34	1.70	2.15
1050	0.3	15.6	237.68	-36.08	-15.07	-0.39	1.86	2.41

Table E.1 (Continued)

DR_0	=	range correction based on the measured refractivity profile.
DR_7, DR_8, DR_9	=	error in range correction (DR_0 minus the corrections based on the measured profile with different cutoff heights at 15,000 ft, 30,000 ft, and 60,000 ft, respectively).
DR_{10}	=	error in range correction (DR_0 minus the corrections based on the combination of the measured profile with a cutoff height at 30,000 ft and the mean profile above 30,000 ft.
DR_{11}	=	error in range correction (DR_0 minus the corrections based on the combination of the measured profile with a cutoff height at 15,000 ft, the mean profile above 30,000 ft, and the exponential fitting between 15,000 and 30,000 ft.

Table E.1 (Continued)

T+Time (sec)	E (deg)	R (10^6 ft)	DE_0 (mils)	DE_7 (mils)	DE_8 (mils)	DE_9 (mils)	DE_{10} (mils)	DE_{11} (mils)
20	7.6	0.07	0.69806	0.00	0.00	0.00	0.00	0.00
30	17.3	0.08	0.46533	0.00827	0.00	0.00	0.00	-0.00246
40	28.4	0.09	0.35621	0.03171	0.00492	0.00	-0.00023	-0.00144
60	40.8	0.16	0.31431	0.02994	0.01381	0.00111	-0.00119	-0.00150
70	41.4	0.21	0.33016	0.02119	0.00942	0.00015	-0.00127	-0.00150
80	40.8	0.27	0.35199	0.01708	0.00757	0.00009	-0.00106	-0.00124
90	39.6	0.34	0.37615	0.01452	0.00644	0.00008	-0.0009	-0.00106
100	38.4	0.42	0.40108	0.01272	0.00564	0.00007	-0.00079	-0.00092
120	36.0	0.60	0.44827	0.01021	0.00453	0.00006	-0.00063	-0.00074
140	34.1	0.83	0.49007	0.00856	0.00379	0.00005	-0.00053	-0.00062
160	32.5	1.10	0.52501	0.00725	0.00321	0.00004	-0.00045	-0.00053
180	31.4	1.46	0.55208	0.00609	0.00270	0.00004	-0.00037	-0.00044
200	30.6	1.87	0.57351	0.00519	0.00230	0.00003	-0.00032	-0.00037
300	26.9	3.89	0.67533	0.00390	0.00172	0.00002	-0.00024	-0.00028
400	23.4	5.81	0.79318	0.00416	0.00184	0.00002	-0.00026	-0.00030
500	19.9	7.59	0.94849	0.00534	0.00236	0.00004	-0.00032	-0.00038
600	16.4	9.26	1.16199	0.00785	0.00346	0.00006	-0.00047	-0.00055
700	12.9	10.8	1.47865	0.01336	0.00586	0.00011	-0.00078	-0.00093
800	9.3	12.3	2.01251	0.0278	0.01207	0.00029	-0.00154	-0.00187
840	7.9	12.9	2.33197	0.03962	0.01706	0.00044	-0.00213	-0.00264
880	6.5	13.4	2.78141	0.06018	0.02558	0.00075	-0.0031	-0.00392
920	5.1	13.9	3.42577	0.09659	0.04016	0.00130	-0.00469	-0.00614
960	3.6	14.5	4.41053	0.16282	0.06513	0.00232	-0.00725	-0.01017
1000	2.1	15.0	6.25950	0.29134	0.10822	0.00405	-0.01139	-0.01841
1050	0.3	15.6	11.00539	0.47737	0.1586	0.00588	-0.01590	-0.03317

Table E.1 (Continued)

DE_0	=	elevation angle correction based on the measured refractivity profile.
DE_7, DE_8, DE_9	=	errors in elevation angle correction (DE_0 minus the corrections based on the measured profile with different cutoff heights at 15,000 ft, 30,000 ft, and 60,000 ft, respectively).
DE_{10}	=	error in elevation angle correction (DE_0 minus the corrections based on the combination of the measured profile with a cutoff height at 30,000 ft and mean profile above 30,000 ft).
DE_{11}	=	error in elevation angle correction (DE_0 minus the corrections based on the combination of the measured profile with a cutoff height at 15,000 ft, the mean profile above 30,000 ft, and the exponential fitting between 15,000 ft and 30,000 ft).

Table E.2 The Differences Between Refraction Corrections Based on the Profiles with Different Cutoff Heights and the Original Profile (Radar 213002, Pillar Point, Op 6290, July 15, 1976)

T+Time (sec)	E (deg)	R (10^6 ft)	DR_0 (ft)	DR_7 (ft)	DR_8 (ft)	DR_9 (ft)	DR_{10} (ft)	DR_{11} (ft)
57	3.5	1.09	106.42	-35.04	-12.71	-1.10	1.33	0.62
60	3.9	1.08	95.51	-32.41	-11.71	-0.71	1.39	0.75
64	4.7	1.08	83.37	-29.04	-10.38	-0.34	1.35	0.79
68	5.5	1.08	73.81	-26.23	- 9.32	-0.14	1.4	0.92
72	6.3	1.07	65.88	-23.81	- 8.45	-0.04	1.36	0.92
76	7.2	1.07	59.18	-21.72	- 7.73	-0.02	1.26	0.86
80	8.0	1.07	53.48	-19.88	- 7.09	-0.02	1.16	0.80
90	10.3	1.07	42.62	-16.16	- 5.79	0	0.96	0.68
100	12.7	1.07	35.00	-13.44	- 4.83	0	0.80	0.57
120	17.9	1.09	25.36	- 9.85	- 3.55	0.01	0.60	0.43
140	22.8	1.16	20.23	- 7.89	- 2.84	0.01	0.48	0.35
160	26.9	1.29	17.38	- 6.79	- 2.45	0.01	0.42	0.30
180	29.9	1.52	15.78	- 6.18	- 2.23	0.01	0.38	0.27
200	31.5	1.84	15.08	- 5.91	- 2.14	0	0.36	0.26
300	29.6	3.66	15.95	- 6.25	- 2.25	0.01	0.38	0.27
400	25.7	5.50	18.09	- 7.07	- 2.55	0.01	0.43	0.31
500	21.9	7.25	21.02	- 8.19	- 2.95	0.01	0.50	0.36
600	18.2	8.89	25.03	- 9.73	- 3.51	0	0.59	0.42
700	14.5	10.4	30.97	-11.96	- 4.30	0	0.72	0.51
800	10.9	11.9	40.62	-15.46	- 5.54	0.01	0.93	0.65
840	9.4	12.4	46.40	-17.50	- 6.26	-0.01	1.03	0.72
880	7.9	13.0	54.09	-20.10	- 7.17	-0.01	1.18	0.81
920	6.5	13.5	64.79	-23.52	- 8.35	-0.04	1.35	0.91
960	5.0	14.0	80.21	-27.96	- 9.84	-0.07	1.56	1.03
1000	3.5	14.5	105.25	-33.92	-11.76	-0.11	1.84	1.14

Table E.2 (Continued)

T+Time (sec)	E (deg)	R (10^6 ft)	DE_0 (mils)	DE_7 (mils)	DE_8 (mils)	DE_9 (mils)	DE_{10} (mils)	DE_{11} (mils)
57	3.5	1.09	3.65097	.46534	.14833	.01144	-0.01566	-0.0014
60	3.9	1.08	3.32426	.40109	.13072	.00779	-0.015	-0.00383
64	4.7	1.08	2.96223	.32408	.10745	.00434	-0.01321	-0.00501
68	5.5	1.08	2.66975	.26423	.08879	.00239	-0.01226	-0.00603
76	7.2	1.07	2.20771	.17830	.06134	.00098	-0.00922	-0.00544
80	8.0	1.07	2.02009	.14765	.05127	.00070	-0.00783	-0.00481
90	10.3	1.07	1.64594	.09493	.03345	.00029	-0.00527	-0.00345
100	12.7	1.07	1.36883	.06357	.02258	.00012	-0.00364	-0.00246
120	17.9	1.09	0.99541	.03161	.01132	.00001	-0.00187	-0.00131
140	22.8	1.16	0.78268	.01825	.00655	-.00001	-0.00109	-0.00078
160	26.9	1.29	0.65843	.01172	.00421	-.00001	-0.00071	-0.00051
180	29.9	1.52	0.58643	.00809	.00291	0	-0.00049	-0.00035
200	31.5	1.84	0.55526	.00614	.00221	-.00001	-0.00037	-0.00027
300	29.6	3.66	0.60562	.00407	.00147	0	-0.00024	-0.00017
400	25.7	5.50	0.71337	.00425	.00153	0	-0.00025	-0.00018
500	21.9	7.25	0.85488	.00533	.00191	-.00001	-0.00032	-0.00023
600	18.2	8.89	1.04290	.00762	.00273	0	-0.00045	-0.00032
700	14.5	10.4	1.31425	.01252	.00446	.00002	-0.00072	-0.00050
800	10.9	11.9	1.74636	.02441	.00862	.00007	-0.00137	-0.00090
840	9.4	12.4	2.00290	.03403	.01193	.00012	-0.00186	-0.00120
880	7.9	13.0	2.34198	.04978	.01727	.00024	-0.00264	-0.00162
920	6.5	13.5	2.81233	.07719	.02631	.00047	-0.0039	-0.00220
960	5.0	14.0	3.48888	.12664	.04186	.00097	-0.00597	-0.00284
1000	3.5	14.5	4.59411	.22460	.07008	.00198	-0.00951	-0.00279